**desert
research
institute**

TRUCKEE CANAL SEEPAGE ANALYSIS IN THE FERNLEY/WADSWORTH AREA

Todd Mihevc
Greg Pohll
Rich Niswonger
Elizabeth Stevick

JANUARY 2002

ABSTRACT

Leakage from the Truckee Canal in the greater Fernley area may contribute significant recharge to the aquifer in that area. Previous efforts to quantify recharge from seepage losses were plagued by uncertainty in the measurement techniques. The focus of this investigation was to estimate seepage losses by monitoring surface and subsurface temperatures. Those data are utilized in a numerical simulation that models both energy and fluid flux. The advantage of this technique is that temperatures are fairly easy to measure and they are used as input to the simulation as well as verification of how well the simulation matches the observed conditions. Six monitoring sites were chosen along the Truckee Canal in the Fernley area that reflect a range of saturation potential that was determined by an electrical resistivity survey.

The modeling effort at these six sites produced estimates of seepage losses that varied from a low of 0.6 cm/day to a high of 47.8 cm/day. By applying the seepage rates estimated by the model to the appropriate sections of canal it was estimated that the total annual loss in the Fernley area is 11,187 acre-feet (af) or 1,614 af/y/mi. of canal. This estimate compares fairly well to estimates of seepage losses in this area made by other techniques.

CONTENTS

LIST OF FIGURES

LIST OF TABLES

INTRODUCTION

Leakage from the Truckee Canal between Wadsworth and East Fernley may make significant contributions to the aquifer in the Fernley area. Previous efforts were plagued by uncertainty in the measurment techniques and poor conceptualization of the subsurface system. Under the guise of the DRI /Washoe County Total Dissolved Solids study (Pohll *et al.,* 2001), substantial resources have been directed towards addressing issues related to possible leakage from the Truckee Canal in the reach between Wadsworth and east Fernley. In particular, two boreholes were drilled adjacent to the canal in early 1999, with the intent of establishing depth to water at these locations. Somewhat surprisingly, water table location exceeded the depth capability of the auger rigs used for this operation (>110 ft). While this information provided new information on the location of the water table in this area, it did not allow a Darcy's Law approach for calculating fluid flux from the canal, necessitating alternate approaches and additional resources for the effort.

The primary objective of this study component was to characterize the fluid flux from the Truckee Canal and adjacent laterals into underlying aquifers. Several methods have been proposed over the past two years. This research incorporated a variation on some of these, wherein thermal-based analysis, a ponding experiment and geophysical techniques were integrated. The focus of these studies was to:

1. Determine potential zones of seepage along the Truckee Canal for proper placement of thermocouple arrays.
2. Use heat pulses as a means to quantify the seepage loss from the Truckee Canal. Multiple thermocouple arrays will be utilized to assess the spatial variability in seepage loss.
3. Perform a ponding experiment along one section of a lateral canal to both determine the seepage loss from the lateral canals and to heat pulse methodology to determine fluid flux.

SITE SELECTION

Several factors dictated where the monitoring site would be located along the Truckee Canal. The main scientific consideration was to locate monitoring sites to cover a range of soil saturation potential described by Mike Widmer (Widmer, 2000), who analyzed resistivity data collected in a geophysical survey by Ehni Enterprises. It was also important to find monitoring sites that had good spatial distribution throughout the town of Fernley. Practical considerations include the ability to get the drilling rig close to the canal to facilitate drilling the angle boreholes under the canal. Figure 1 shows the locations for the monitoring sites and the moisture potential as interpreted by Widmer (Widmer, 2000) using the resistivity survey.
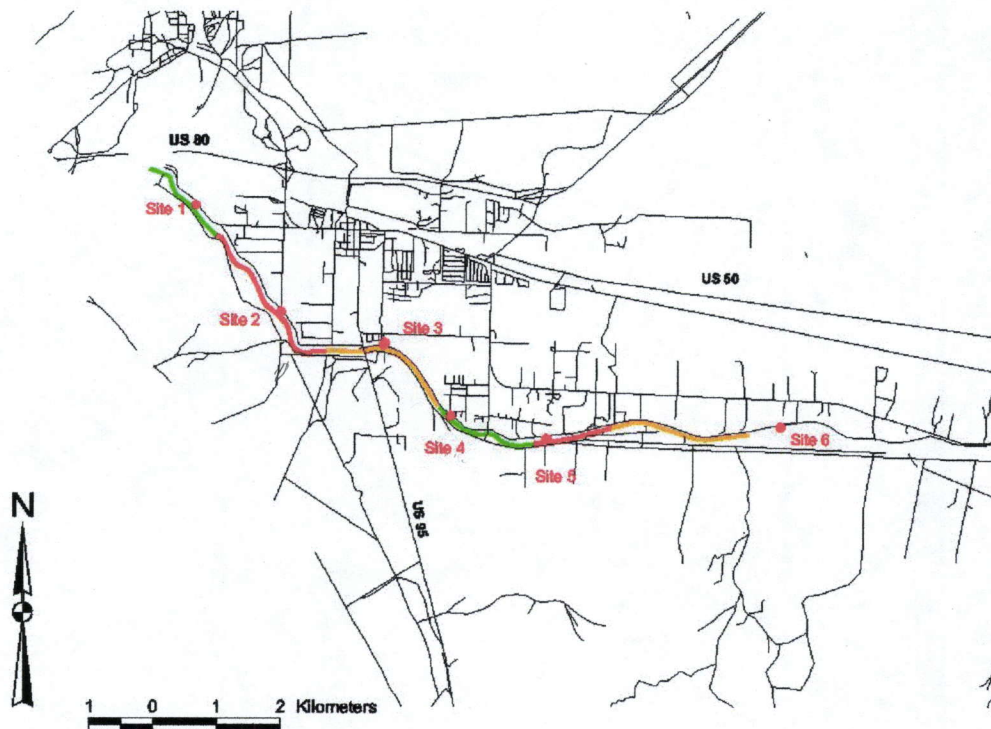
Figure 1.   Location of the temperature monitoring sites and the saturation potential determined by the geophysical survey along the Truckee Canal. The red zones are areas of high saturation potential, yellow indicates moderate saturation potential, and green indicates low saturation potential.

INSTRUMENTATION

Instrumentation for each of the monitoring sites consist of a Campbell Scientific CR10X datalogger and approximately 11 thermocouples. Thermocouples were constructed in the laboratory using Omega copper-constantan insulated thermocouple wires that were cut to 40-foot lengths. The copper-constantan junctions were soldered and dipped in Plastidip, a rubber coating to electrically insulate the junction from the environment. The datalogger has the capability of measuring 12 thermocouples, one reference and 11 sensors, however, where the Plastidip or insulation became abraded during installation, the sensor required an extra input channel to eliminate grounding potential, thus reducing the total number of sensors that could be installed at those particular sites.

At each monitoring site thermocouples were installed in two boreholes, one bored vertically adjacent to the canal and one drilled at an angle beneath the canal. The boreholes were 5.5-inches in diameter and were drilled with a Giddings auger-drilling rig. The depth of the boreholes ranged from 15 feet (ft) to 25 ft, which was primarily controlled by the geologic material encountered. Thermocouples were attached to 3/16-inch-diameter dowels to ensure proper depth of burial. Once the array of thermocouples was attached to the dowel, it was inserted into the borehole, which was backfilled with native material and several bentonite pellet plugs to prevent preferential water movement along the borehole. The third array of sensors was installed in the canal by attaching the thermocouples to a broomstick. The broomstick was pounded into holes made by driving metal pipe and then removing it.

2

The sensor arrays in the channel were the most important for modeling purposes, the most difficult to install, and have the greatest uncertainty with respect to the exact position of each sensor in the array. Thermocouple wire was brought into the datalogger enclosure through an insulated PVC pipe, with the excess buried in the soil directly below the datalogger. These steps were necessary to decrease temperature gradients in the thermocouple wire that could affect measured temperature.

Temperature measurements were saved every 15 minutes using an average of five measurements for each sensor. For modeling purposes, those 15-minute measurements were averaged every hour by post-processing. Using hourly averages reduced noice in the temperature data, which allows for a more accurate model inversion. A complete graph of the data collected at each site is presented in Appendix A. The temperature data did show diel variation of as much as 0.5 degrees, which was probably the result of high temperature of the near-surface thermocouple wire. To remove this variation, the data were post-processed by first examining the temperature signal of the deepest sensor. The deepest sensor at each site was used because temperature changes very slowly at depth and any measured changes would be the result of the high temperatures of the wires at the near surface. Smoothing fitting routines were applied to the observed data to produce new datasets without noise. An example of the pre- and post-processed data is shown in Figure 2.
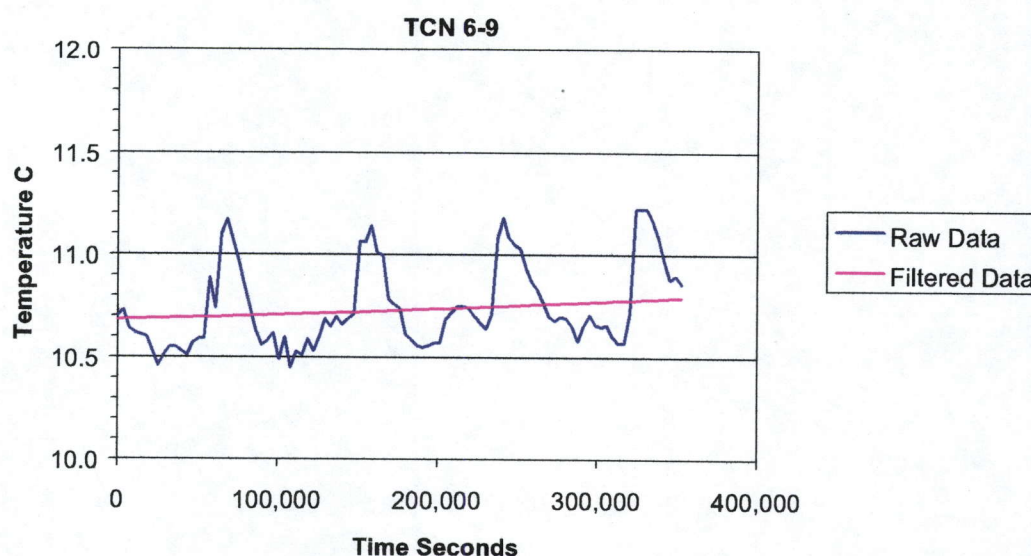
Figure 2.   Example of raw data from TCN 6-9 showing diurnal variation due to high temperature of the near-surface thermocouple wire and the filtered data with the diel variation removed.

NUMERICAL SIMULATION

Heat can be used as a tracer as surface water infiltrates into the ground. The two main mechanisms for heat transfer from a body of water to the underlying sediments are conduction and advection. The transfer of heat by conduction occurs as diffusive molecular transfer between the streambed surface and the underlying sediments. Advective heat transfer occurs from the movement of water. Using heat as a tracer for ground water recharge has the

3

advantage, as it is an easy parameter to measure and can be used in conjunction with numeric models to determine hydraulic parameters and estimate fluid flux rates.

The numerical model VS2DH (Healy and Ronan, 1996) was used to estimate seepage losses along the Truckee Canal in Fernley. VS2DH simulates the flow of liquid water and energy in a two-dimensional variably saturated domain. Energy or heat transport is described using the advection/diffusion equation expressed in terms of water temperature (Equation 1).

$$\frac{\partial[\theta C_w + (1 - \phi)C_s]T}{\partial t} = \nabla \cdot K_T(\theta)\nabla T + \nabla \cdot \theta C_w D_H \nabla T - \nabla \cdot C_w T v + q C_w T* \qquad (1)$$

where C_W is heat capacity of water [ML^{-1} T^{-2} °C^{-1}], θ is porosity [-] (nondimensional), C_S is heat capacity of the dry solid grains [ML^{-1} T^{-2} °C^{-1}], K_T is the thermal conductivity of the water and solid matrix [ML T^{-3} °C^{-1}], D_H is the thermomechanical dispersion tensor [L^2 T^{-1}], v is water velocity [L T^{-1}], q is rate of fluid source [T^{-1}], and T* is temperature of fluid source [°C]. Water movement in the unsaturated zone is described by the Richardson Equation (Equation 2).

$$C(\psi, x)\frac{\partial h(\mathbf{x}, t)}{\partial t} = \nabla \cdot [\mathbf{K}(\psi, \mathbf{x}) \cdot \nabla h(x, t)] \qquad (2)$$

where t is time, x is the vector of spatial dimension: $C(\psi, x)$ is the specific moisture capacity [L^{-1}], defined as the derivative $d\theta/d\psi$, which is the slope of the moisture retention curve; θ is the volumetric moisture content (water content), ψ is the pressure head [L], h is the toal head [L], equal to $\psi + z$, and $K(\psi, x)$ is the hydraulic conductivity tensor [L T^{-1}]. These two equations are solved sequentially within an iterative framework (Prudic and Thodal, 1998).

For our application, we use measured water and air temperature as input into the model. The air temperature was used as a surrogate for soil temperature. The simulated temperatures are used in the model optimizer and for visual verification of how well the model simulates the observed conditions.

PEST, a model independent parameter estimator was used in conjunction with VS2DH to optimize two hydraulic parameters, horizontal hydraulic conductivity and anisotropy. The anisotropy is defined as the ratio of the horizontal hydraulic conductivity (K_h) and the vertical hydraulic conductivity (K_v): K_h/K_v. PEST was set up to run VS2DH, take the output, which consists of estimated temperatures at model nodes at predetermined simulation times, and compare those temperatures to observed temperatures. PEST then modified the hydraulic parameters and re-simulated VS2DH with the new parameters. This process continued until the discrepancies between the model-generated values and the measured values were reduced to a minimum.

With respect to the application used here, only select thermocouples were used with the PEST optimization. Generally, sensors that were installed beneath the canal responded very well to changes in water temperature and were utilized in the PEST optimization. Then some of the sensors located in the adjacent boreholes were used for the PEST optimization depending on their response to changes in water temperature. Generally, the further from the canal, the less likely it is that those sensors would respond to changes in water temperature.

One can take advantage of the flow symmetry by only simulating one-half of the canal section. Therefore, each model domain represents the canal from its midpoint to the

4

canal bank where the intrumentation is installed. Although individual site models were modified slightly to represent the site geometry, Figure 3 shows a general representation of the model domain. The domain extends from the ground surface to approximately   40 m below ground surface, which is the approximate location of the water table in this region. The domain extends laterally from the centerline of the canal to a distance of approximately 33 m to remove any potential boundary condition effects on the model simulations.

Boundary Conditions

The numerical model requires boundary conditions as input parameters. Hydraulic boundaries consist of no-flow vertical boundaries representing the axis of symmetry and the vertical boundary outside of the canal section. The lower boundary is simulated with a pressure head of zero to represent the water table conditions. The upper boundary varies between a specified head to represent the canal section and no-flow conditions above the fluid level in the canal. Thermal boundaries are represented by no energy flow along both vertical boundaries. The lower boundary is represented as a constant temperature of 12°C to represent the relatively constant temperature at this depth. The upper boundary is represented by a specified temperature condition with measured water temperatures being used for the channel section and measured air temperatures being used for the soil temperatures.

Legend
No-Flow, Specified Soil Temperature
Specified Head, Specified Fluid Temperature
No-Flow, No Energy Flux
Specified Head, Constant Fluid Temperature
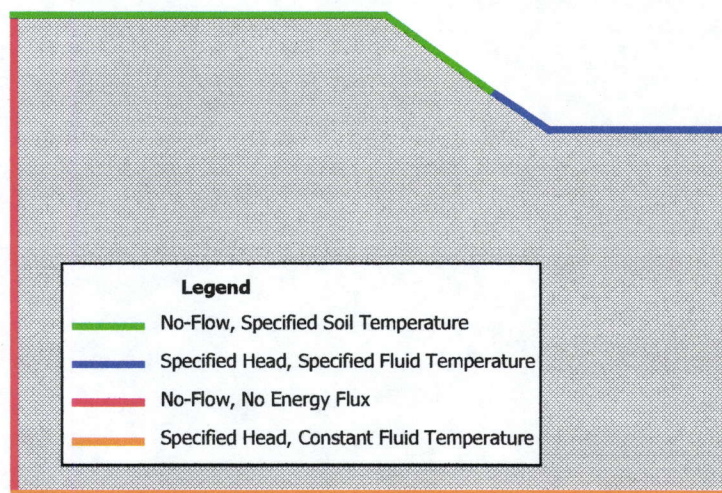
Figure 3.   Generalized model domain used in VS2DH simulations.

Results

Site 1

Site 1 is the westernmost monitoring site in the study area (See Figure 1). The thermocouple arrays consist of three sensors driven in the canal, two inserted in the angle hole beneath the canal and four sensors inserted in the vertical hole adjacent to the canal (Figure 4). While drilling the vertical borehole at site 1 the material encountered was mainly sandy to silty soils. The borehole was dry to 6 ft BLS. Moisture content increased with depth but no standing water was observed in the borehole. This site was located in an area as described by the geophysical survey as having low moisture potential.
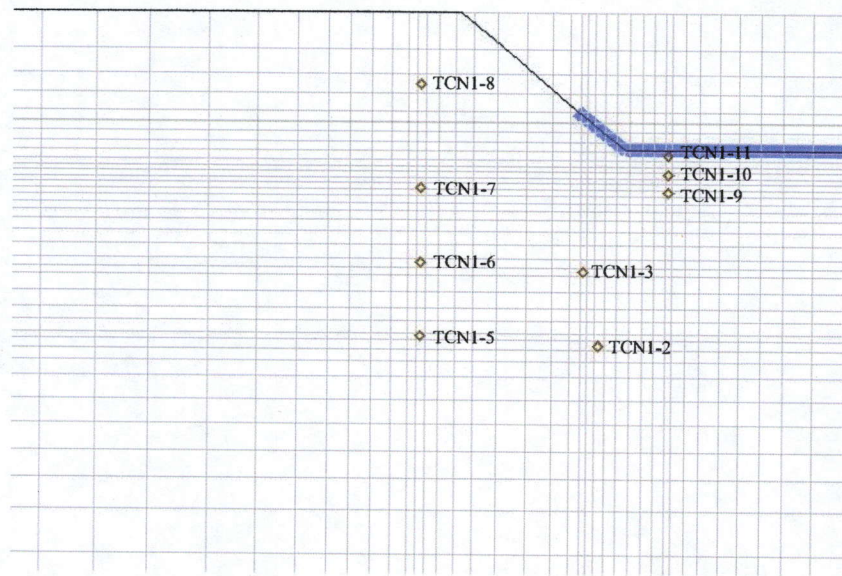
Figure 4.   Location of thermocouples and model grid at Site 1.

Site 1 Model

The model domain for site 1 consists of a 63 by 78 cell matrix. The data used for this simulation came from a 19-day period from April 22, 2001 to May 10, 2001. Figure 5 is a plot of the water temperature and the temperatures of the sensors beneath the canal for the modeling period. The water temperature varied between 8.5 and 19.5 degrees, which provides good variability during the modeling period. Of interest in this plot is that the temperature signal from the canal water is not only attenuated in magnitude from surface to depth but also that the lag time that occurs as a warm pulse moves down through the sediments.
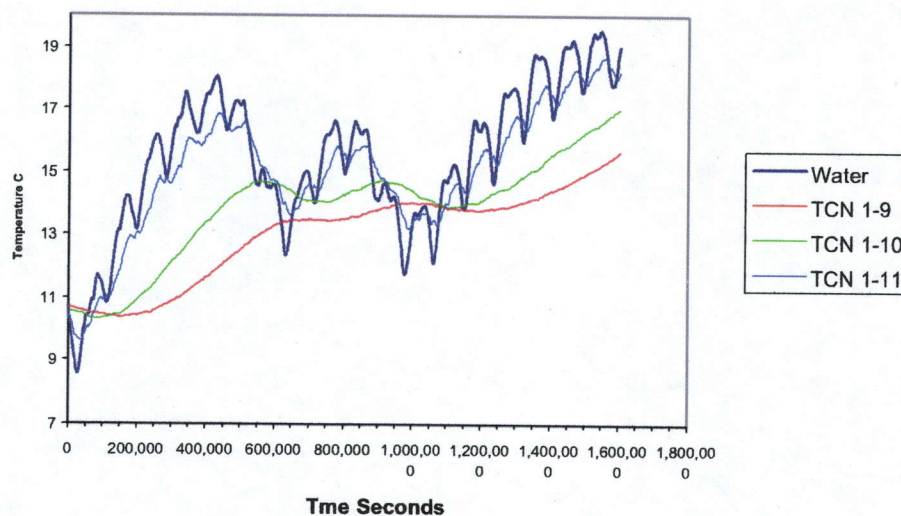
Figure 5.   Measured water and subsurface temperatures at Site 1. TCN 1-11 is the shallowest sensor, TCN 1-10 is intermediate, and TCN 1-9 is the deepest sensor.

6

During optimization, a total of 41 model calls were made. The optimal horizontal hydraulic conductivity was determined to be 2.8 x 10^{-6} m/s and the optimal anisotropy was determined to be 0.38, which gives a vertical hydraulic conductivity of 7.3 x 10^{-6} m/s. Comparisons between measured temperatures and simulated temperatures for the thermocouples beneath the channel and in the angle hole can be seen in Figures 6 through 10. Generally, there is good agreement between the measured temperature and the modeled temperature, however, the further from the channel, the worse the agreement is. This is especially true of the comparison of the measured and simulated temperatures in the horizontal hole adjacent to the canal.

Figure 6.   Measured and simulated temperatures for TCN 1-11.

Figure 7.   Measured and simulated temperatures for TCN 1-10.

Figure 8.   Measured and simulated temperatures for TCN 1-9.

Figure 9.   Measured and simulated temperatures for TCN 1-3.

Figure 10. Measured and simulated temperatures for TCN 1-2.

The fluid flux from the canal to the groundwater at site 1 is estimated at 20.8 cm/day for the time period simulated. Figure 11 shows the flux and water temperature through the modeled period. In this figure the water temperature is warmer at 400,000 seconds (4.6 days) than it is at 800,000 seconds (9.3 days) but the flux is lower at 400,000 seconds. This is somewhat misleading because the period modeled for site 1 was in April where the ground and subsurface water temperatures were lower. So the flux is not only related to the water temperature but more importantly, to the subsurface temperatures (Constantz et al., 1994).
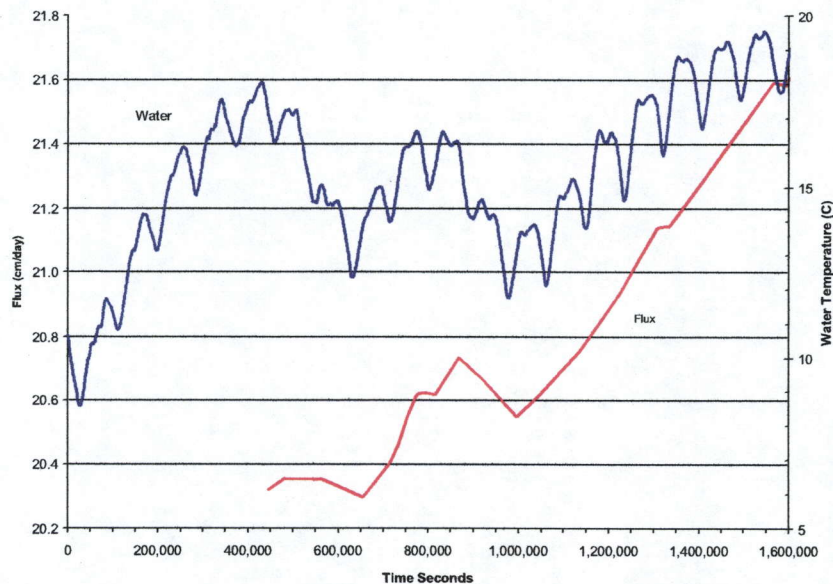
Figure 11. Water temperature and flux rate at Site 1 for the modeled time period.

9

Site 2

Site 2 is located in an area that was defined by the geophysical survey as having high moisture potential (see Figure 1). The thermocouple arrays at site 2 consist of three sensors installed vertically beneath the canal, four sensors in the angled borehole beneath the canal, and three sensors installed in the vertical borehole adjacent to the canal. While drilling the boreholes at this site, moist clay was encountered down to approximately 16 ft; below this depth, dry silty clay was encountered.

Site 2 Model

The domain for Site 2 (Figure 12) consists of a 60 by 48 cell matrix. Temperatures used in the simulation are from the time period April 14 to May 10, 2001, which gives a 27 day simulation period. Comparisons between simulated and measured temperatures for some of the sensors are presented in Figures 13 to 16. Figure 13 shows the comparison of the simulated temperature compared to the observed temperature for TCN 2-3, which is the second sensor from the top in the angle borehole. Although the comparison is slightly off for the early period of the simulation, it compares fairly well at late times. One reason for the early time difference is the initial conditions set up in the model, where the observed temperature was different from the initial temperature. This is even more of an issue in the sensors installed in the vertical borehole adjacent to the canal (Figure 16). Figures 14 and 15 are from the sensors driven beneath the channel. Differences between the observed and measured values in these figures may be the result of uncertainties of modeled depth and actual depth of the sensors.
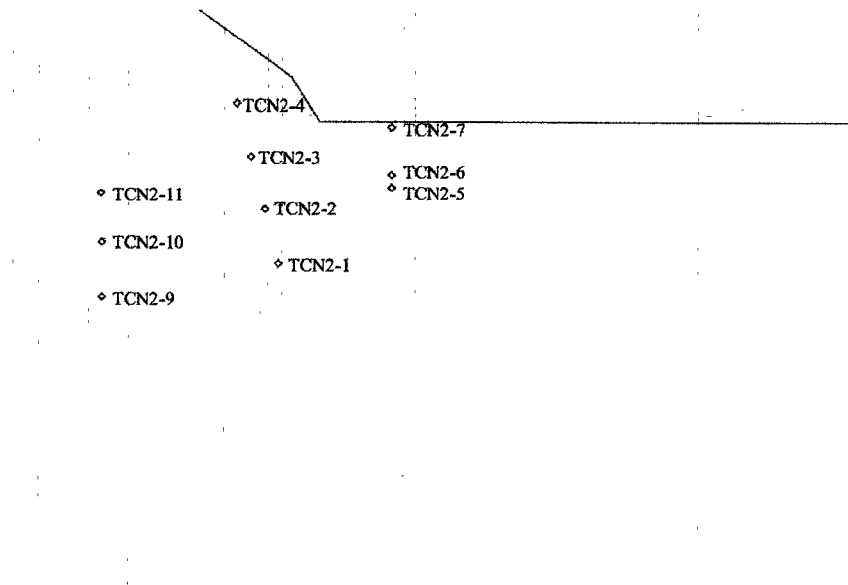
Figure 12.   Location of thermocouples and model grid at Site 2.

10
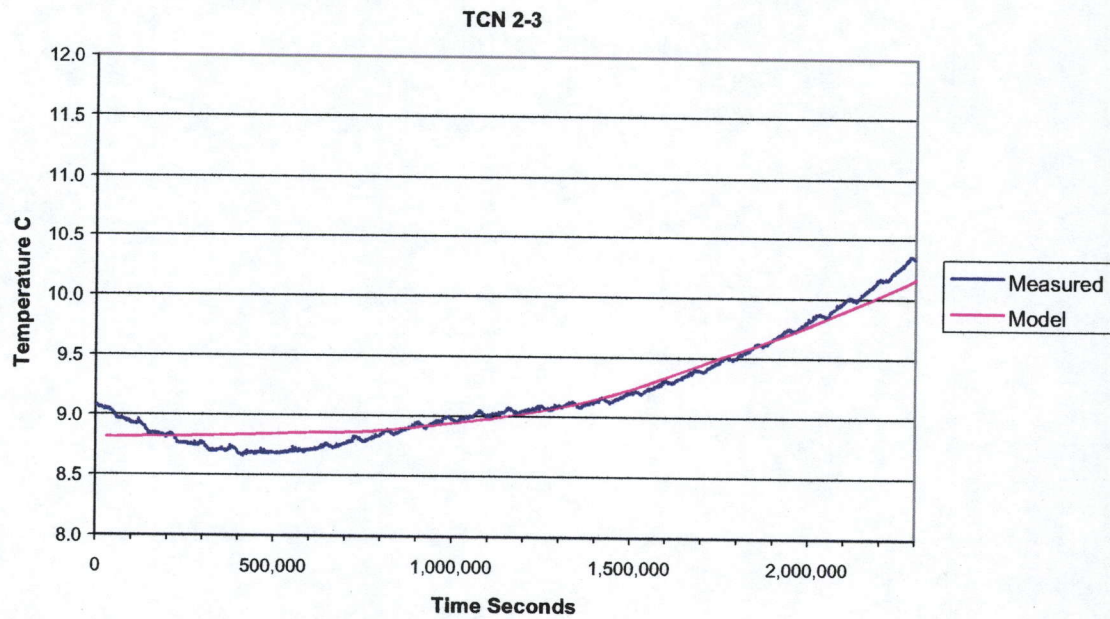
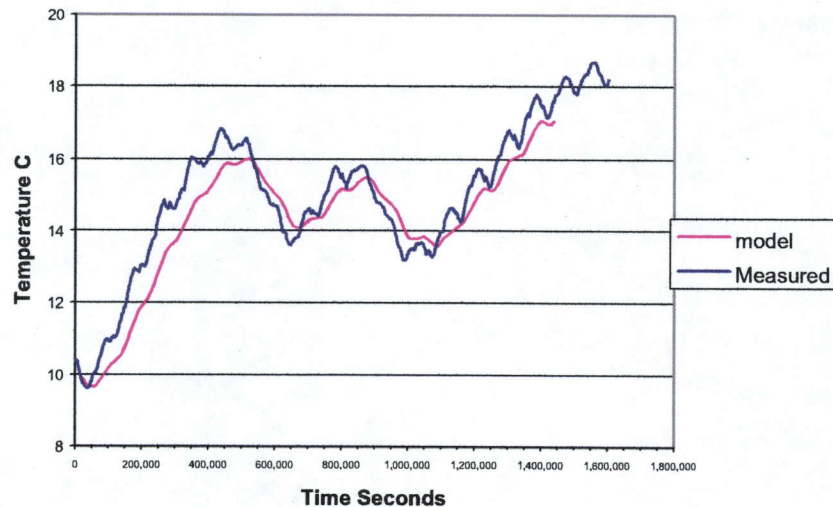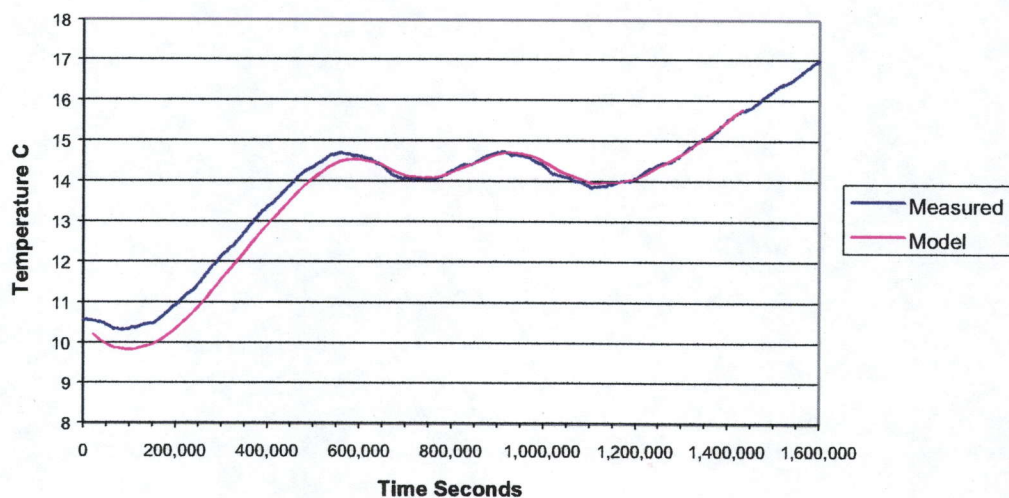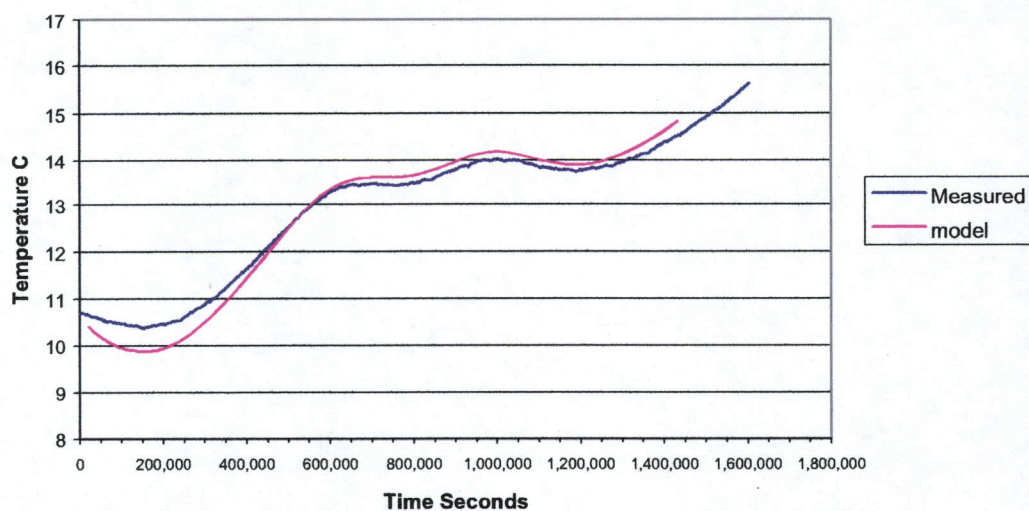Figure 13. Measured and simulated temperatures for TCN 2-3.
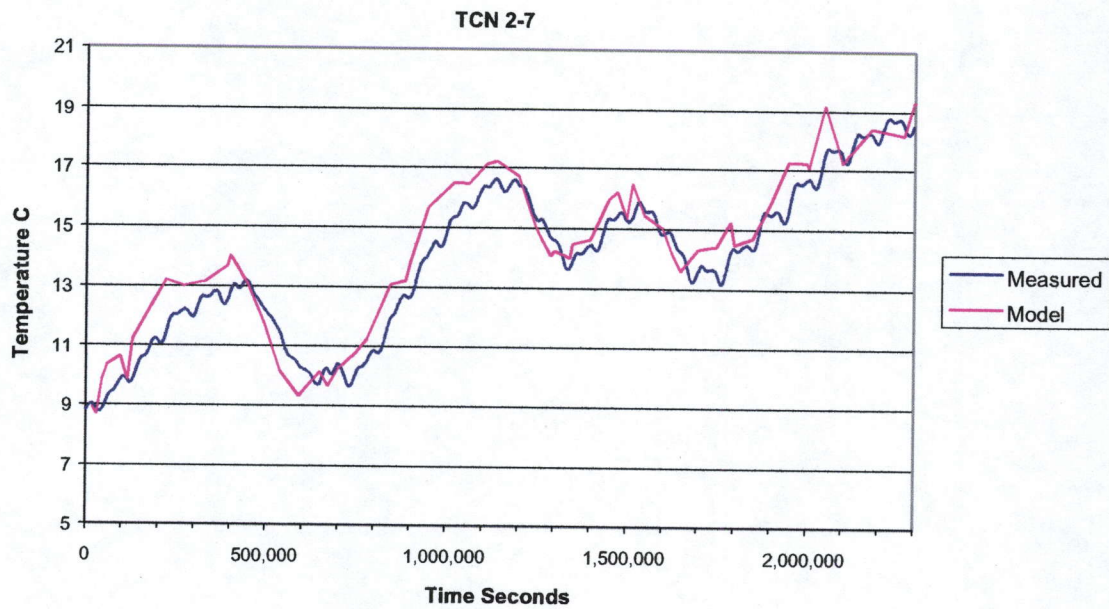
Figure 14. Measured and simulated temperatures for TCN 2-7.

11
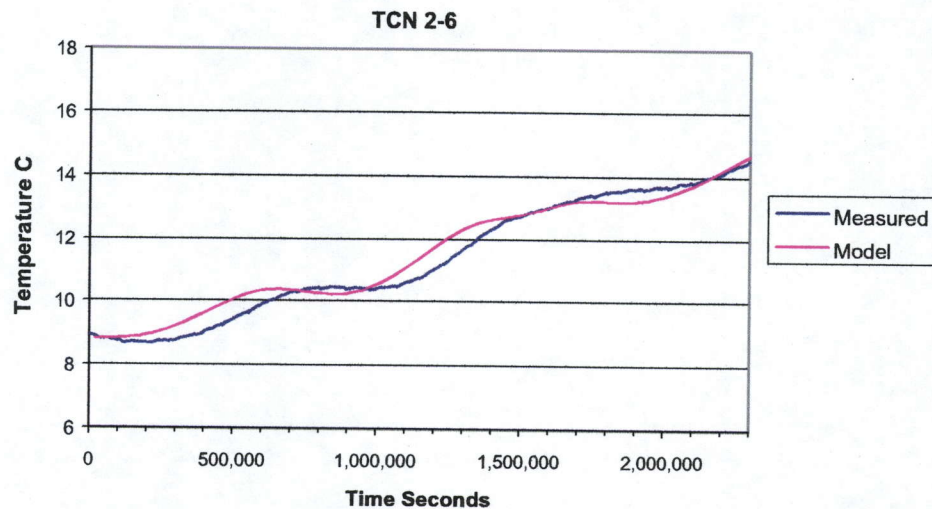
Figure 15. Measured and simulated temperatures for TCN 2-6.

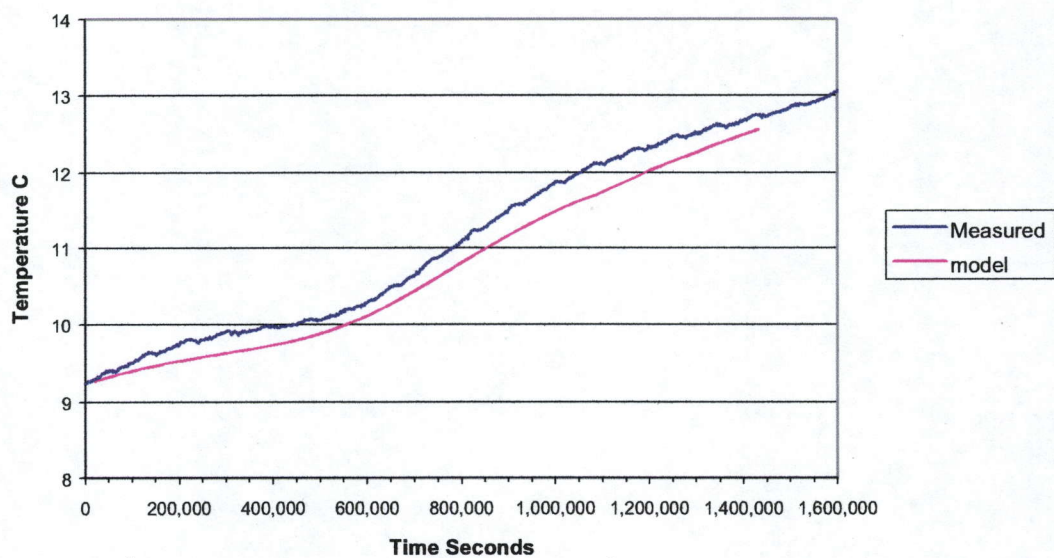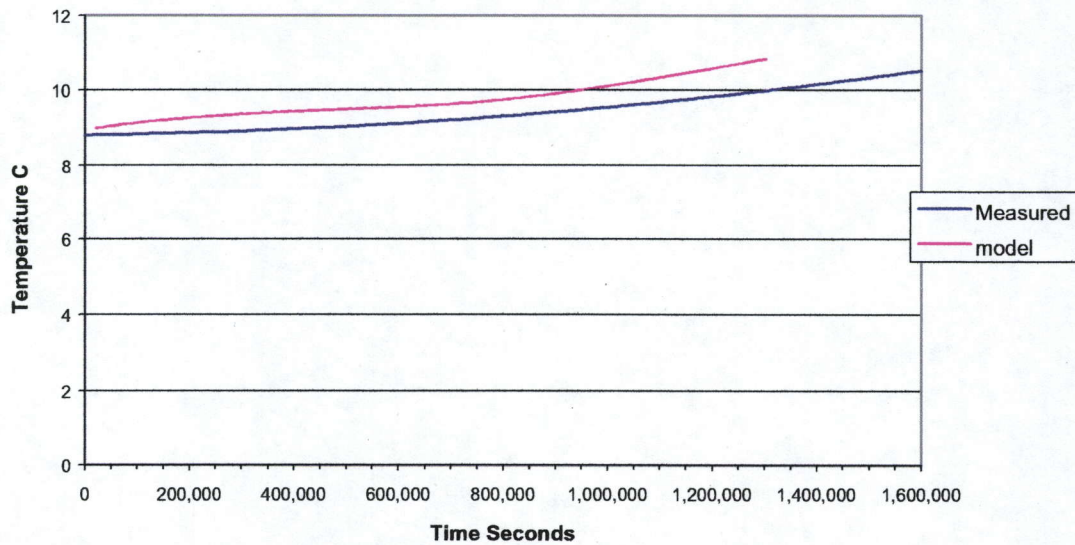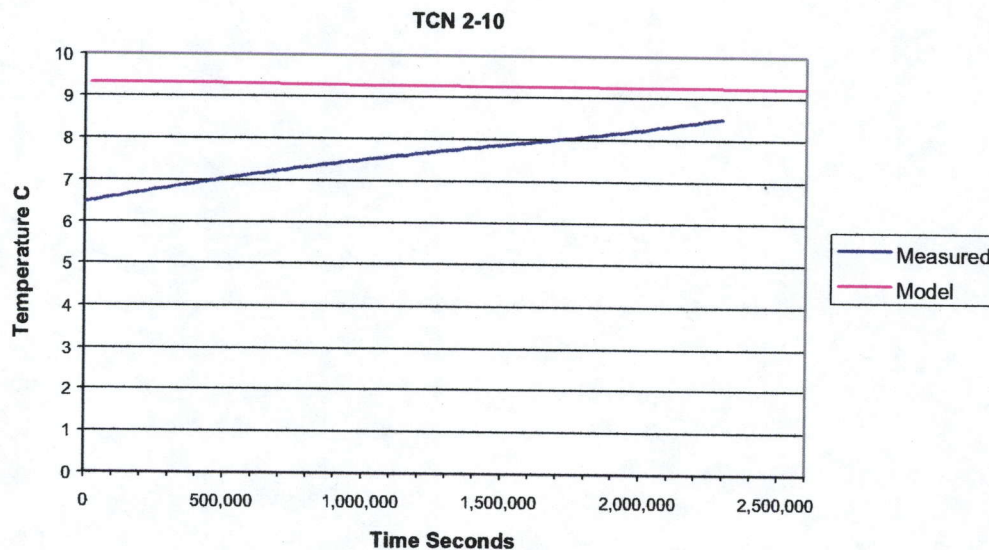Figure 16. Measured and simulated temperatures for TCN 2-10.

The model was run 29 times during optimization, which resulted in an estimate of horizontal hydraulic conductivity of 1.35×10^{-6}, vertical hydraulic conductivity of 4.82×10^{-7} and anisotropy of 0.36. With these hydraulic parameters, the model estimated that the flux from the canal at this location is approximately 3.2 cm/day. Figure 17 shows the estimated flux for the simulation period. The flux at Site 2 was lower than that at Site 1 even though the moisture potential was estimated to be larger than that at Site 1. This is likely the result of the presence of the clays observed at Site 2. The clays were moist in the boreholes drilled at Site 2 but transmit little water.
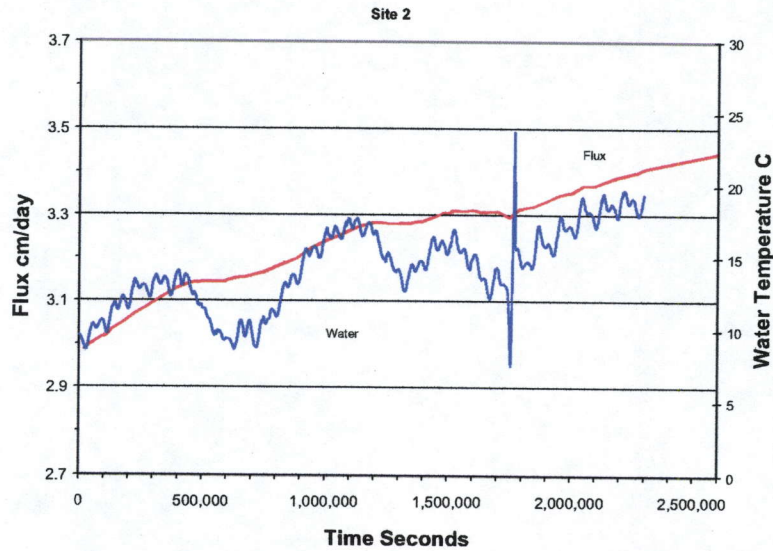
Figure 17. Water temperature and flux rate at Site 2 for the modeled time period.

Site 3

Site 3 is located adjacent to the lateral where the ponding experiment was conducted. It is also located in an area that was considered to have a moderate saturation potential by the geophysical survey (see Figure 1). The sensor arrays consist of three thermocouples driven beneath the canal, three thermocouples installed in the angled borehole beneath the canal, and two thermocouples installed in the vertical borehole adjacent to the canal (see Figure 18). While drilling the boreholes, mostly silty sand material was encountered.
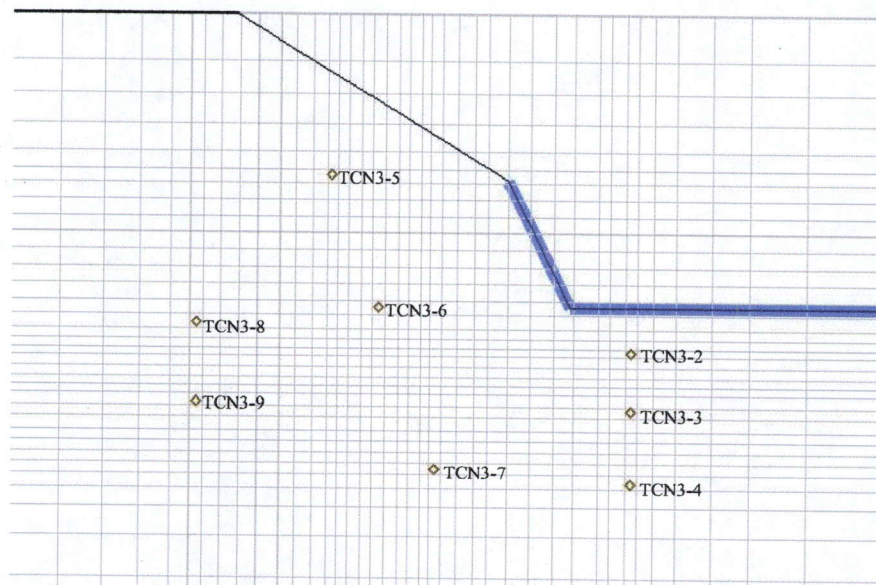
Figure 18. Location of thermocouples and model grid at Site 3.

Site 3 Model

The domain for Site 3 consists of a 68 by 72 cell matrix. The temperature data used for the simulation are from 48 days from the time period between May 17 and July 5, 2001. Comparisons between some of the measured temperatures at Site 3 and simulated temperatures are presented in Figures 19 to 21. Figure 19 shows the comparison between observed temperature and simulated temperature from the deepest sensor beneath the canal. The fairly good agreement observed is not surprising, as the model usually predicts these temperatures fairly well. Figure 20 shows the comparison of temperatures for the middle sensor in the angle borehole and Figure 21 shows the comparison of temperatures from the upper sensor in the vertical borehole. These plots show very good agreement between the measured and simulated values. The significance of this is that the model is not only estimating the vertical hydraulic conductivity well but it is also doing a good job predicting the horizontal hydraulic conductivity.

During optimization, the model was run 19 times, which produced a horizontal hydraulic conductivity of 6.92×10^{-6}, a vertical hydraulic conductivity of 1.68×10^{-6}, and an anisotropy of 0.24. With these hydraulic parameters, the model estimated the average flux at this location over this time period of 16.8 cm/day. Figure 22 shows the estimated flux rate and water temperature over the time of the simulation period.
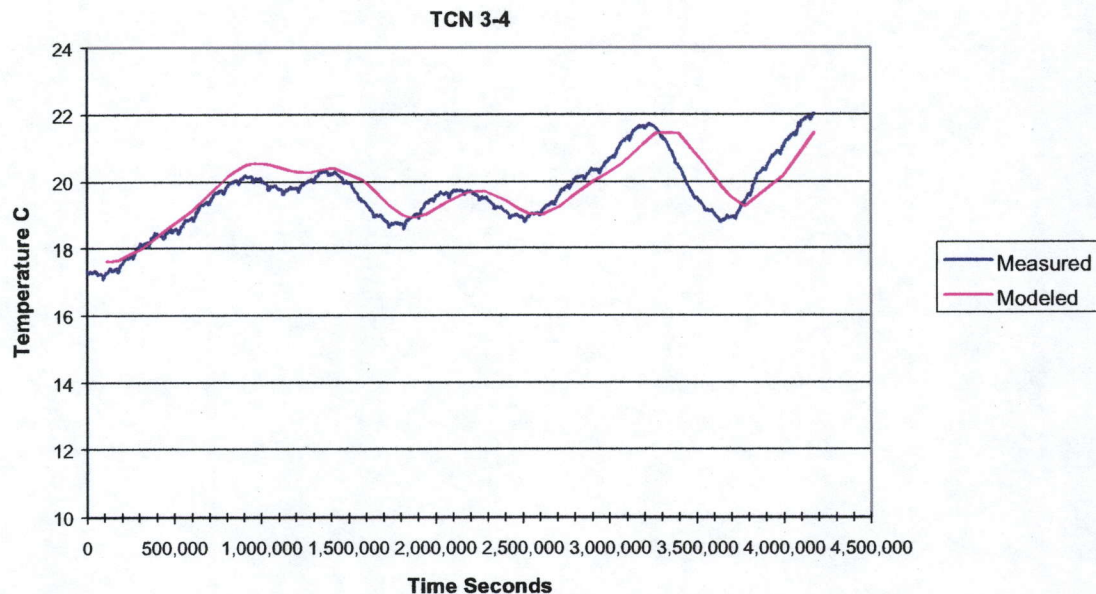
Figure 19.   Measured and simulated temperatures for TCN 3-4.
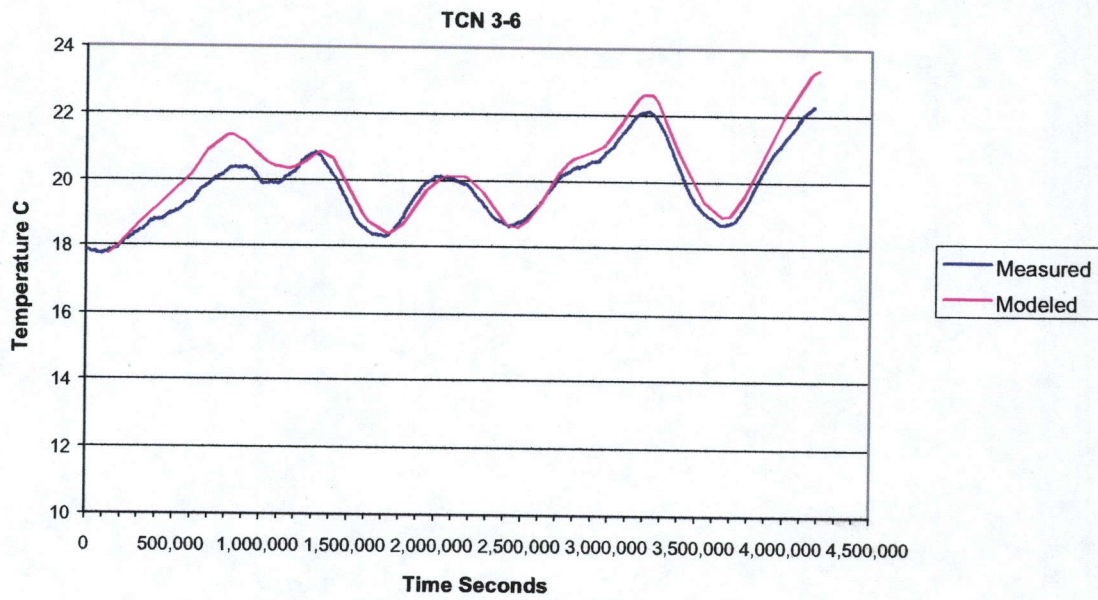
TCN 3-6

Figure 20. Measured and simulated temperatures for TCN 3-6.

TCN 3-8

Figure 21. Measured and simulated temperatures for TCN 3-8.

Figure 22. Water temperature and flux rate at Site 3 for the modeled time period.

Site 4

Site 4 is located in an area that is defined by the geophysical survey as having low saturation potential. This condition was confirmed while drilling the boreholes for the sensors at Site 4 where dry soils were encountered. The sensor arrays at Site 4 consist of four thermocouples driven beneath the canal, two thermocouples installed in the angle borehole beneath the canal and two thermocouples installed in the vertical borehole adjacent to the canal (Figure 23).

Site 4 Model

The temperature data used in the simulation come from a 29-day period from April 9 to May 10, 2001. While comparing model output and measured values it became apparent that the thermocouples driven below the canal slipped up the broomstick during the installation process. Figure 24 is a plot of temperatures from sensors TCN 4-7, 4-8, and 4-9 and estimated temperatures from the simulation at the depths that the sensors were supposed to be installed. The plots for sensors 4-7 and 4-8 lie on top of each other, which suggests that those sensors are installed at the same depth. With the uncertainty of the exact depth of those sensors the modeling effort becomes problematic. Figures 25 and 26 show the measured and simulated temperatures for TCN 4-9 and 4-8, respectively. These figures show good agreement for the measured and simulated temperatures. Figure 27 shows the measured and estimated temperatures for sensor TCN 4-3. There is poor agreement between the two curves in this figure, likely the result of the proximity of the sensor to the water level in the canal. Slight inaccuracies between the real depth and the depth used in the model can have significant effects. After 32 model calls during the optimization, the horizontal hydraulic conductivity was estimated to be 3.6×10^{-7} m/s and the vertical hydraulic conductivity 6.7×10^{-8} m/s. These are the lowest hydraulic conductivity values observed for this project. Figure 28 is a plot of the flux rate and water temperature throughout the simulation period.

16
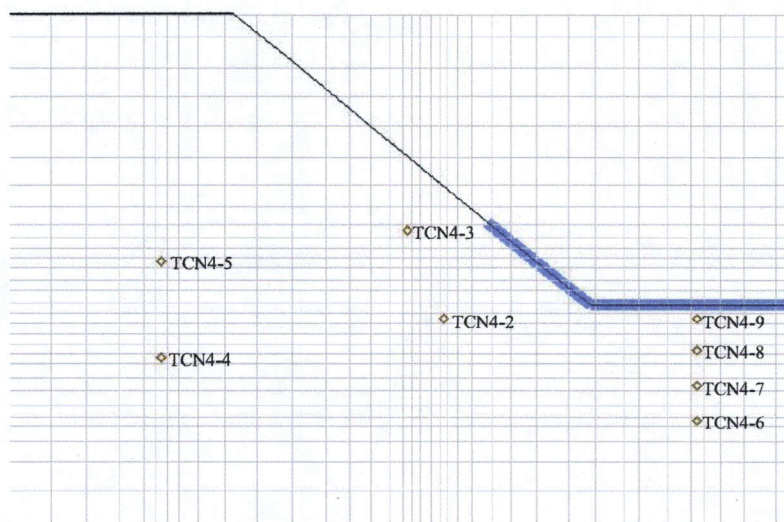
Figure 23. Location of thermocouples and model grid at Site 4.
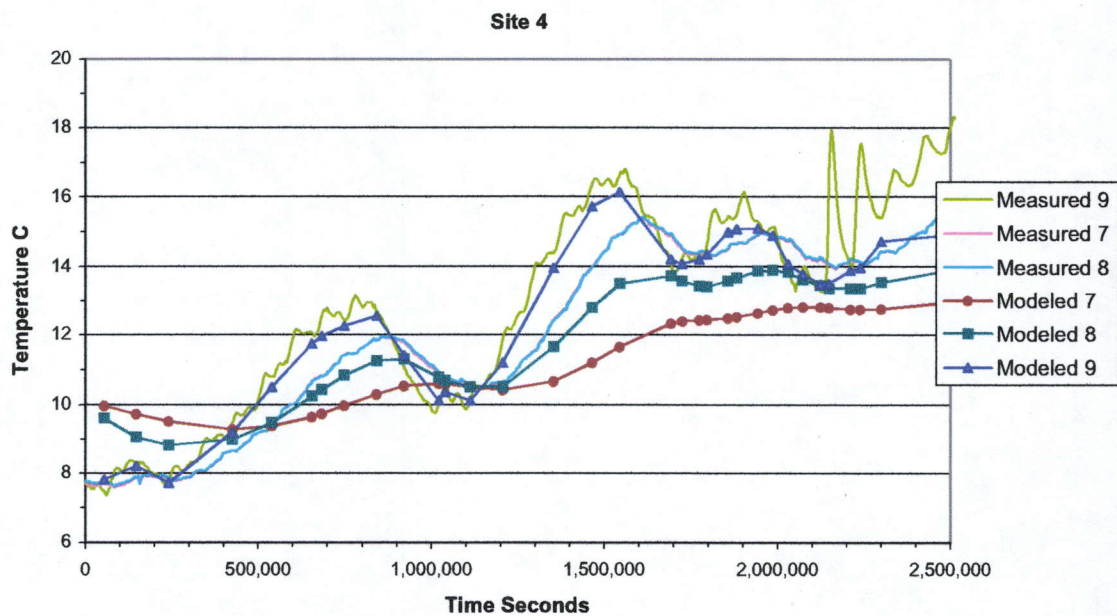
Figure 24. Water temperature and measured and simulated temperatures for the thermocouples installed beneath the canal at Site 4.

17

TCN 4-9

Figure 25. Measured and simulated temperatures for TCN 4-9.

TCN 4-8

Figure 26. Measured and simulated temperatures for TCN 4-8.
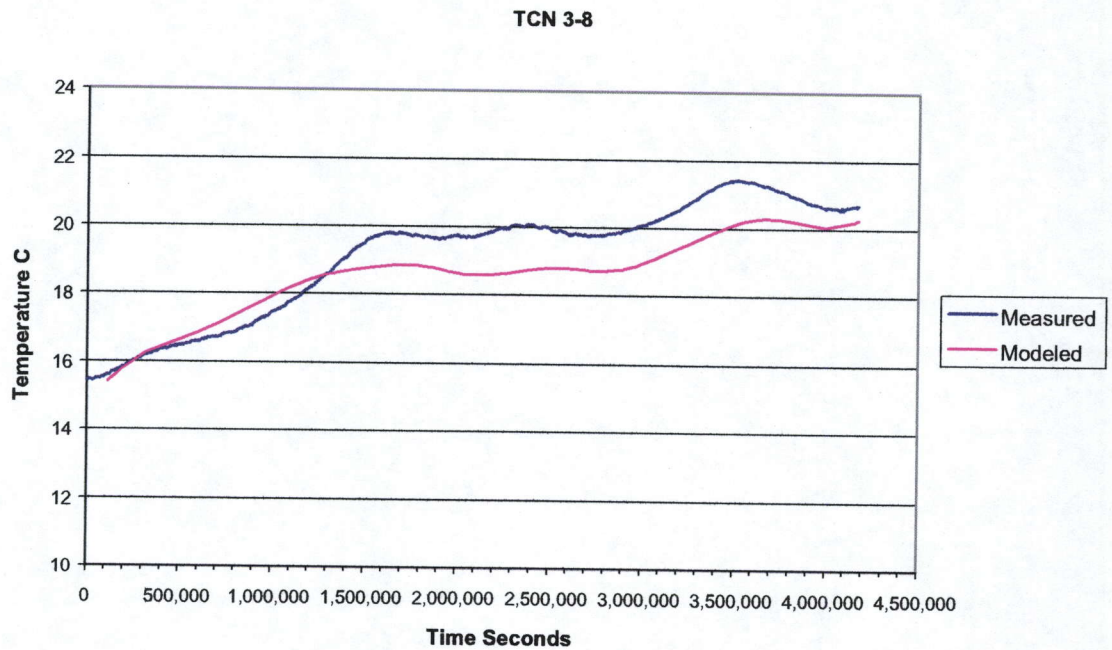
18

TCN 4-3

Figure 27.   Measured and simulated temperatures for TCN 4-3.
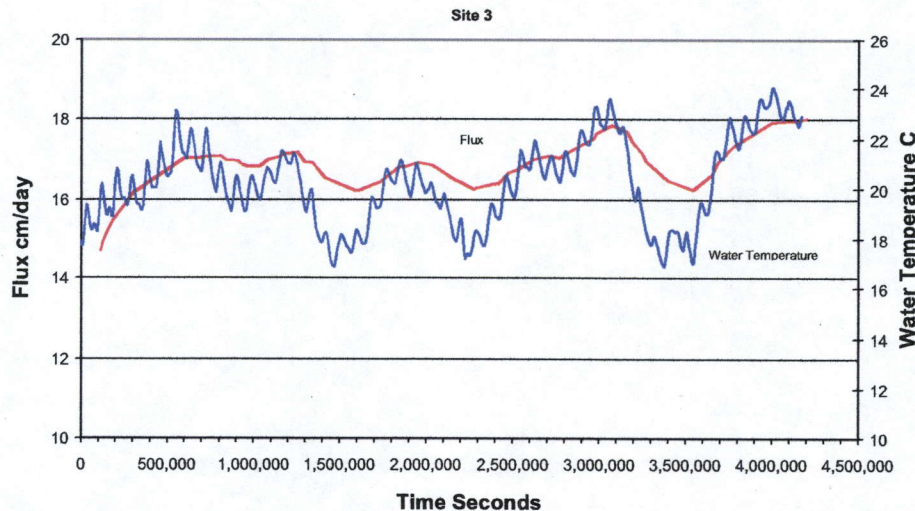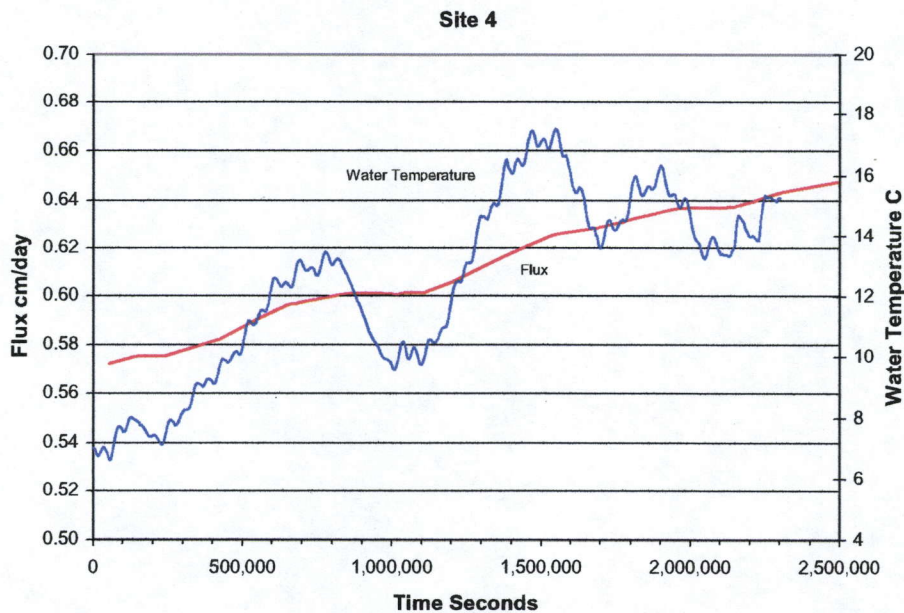
Site 4

Figure 28.   Water temperature and flux rate at Site 4 for the modeled time period.

Site 5

Site 5 is located in an area that is described by the geophysical survey as having a high saturation potential (See Figure 1). The sensor arrays at Site 5 consist of two sensors installed beneath the canal, four sensors installed in the angle borehole beneath the canal, and

19

two sensors installed in the vertical borehole adjacent to the canal. Figure 29 shows the positions of the sensors at Site 5.
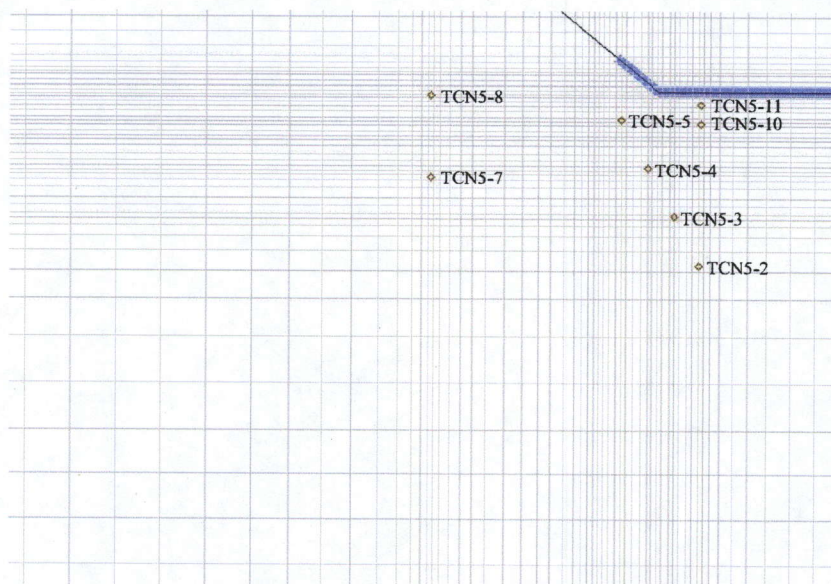
Figure 29. Location of thermocouples and model grid at Site 5.

Site 5 Model

The model for Site 5 was set up with a 72 by 76 cell matrix. Temperature data used in the simulation are from a 35-day period May 31 to July 5, 2001. The data from Site 5 suggest that sensors TCN 5-5, 5-10, and 5-11 responded very well to changes in water temperature, where the other sensors did not. These sensors were used in the optimization with TCN 5-10 having the highest weight. The simulated and measured temperatures for these sensors matched very well (see Figures 30 through 32). However the next lowest sensor in the angled borehole, TCN 5-4 shows a very poor fit for the measured and simulated temperatures, Figure 33. This is likely due to local heterogeneity at this site. The horizontal hydraulic conductivity that the model estimated at this site is 9.8×10^{-6} m/s, the vertical hydraulic conductivity is 3.97×10^{-6} m/s and the anisotropy is 0.41. The average flux rate over the time period of the simulation is 47.8 cm/day, which is the highest flux estimated for this project. Figure 34 shows the flux estimated by the model and the water temperature for the simulation period.

TCN 5-5

Figure 30. Measured and simulated temperatures for TCN 5-5.
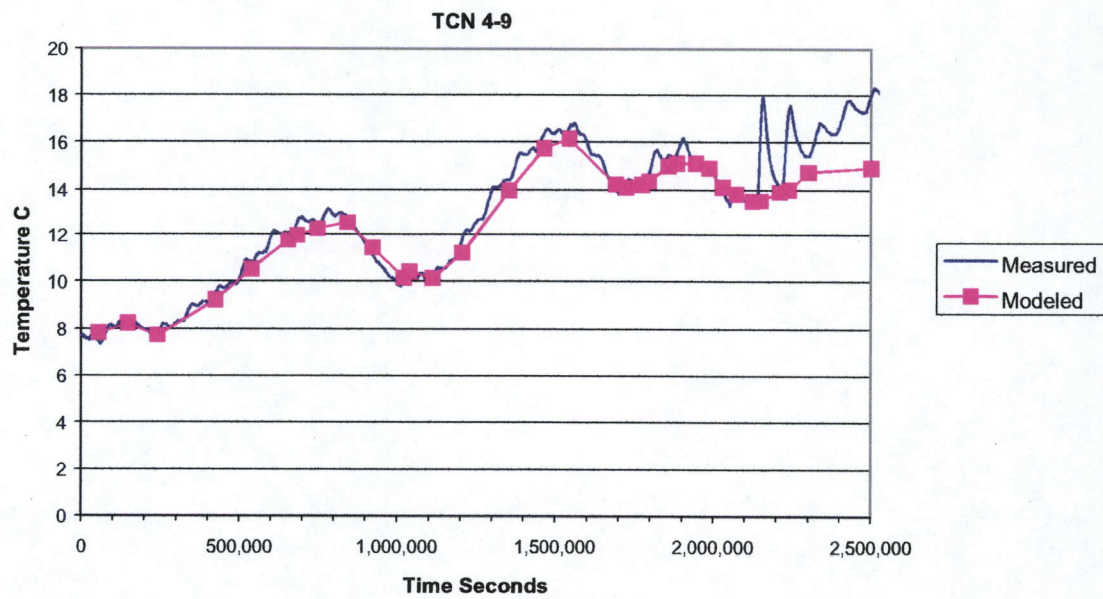
TCN 5-10

Figure 31. Measured and simulated temperatures for TCN 5-10.

Figure 32. Measured and simulated temperatures for TCN 5-11.

Figure 33. Measured and simulated temperatures for TCN 5-4.
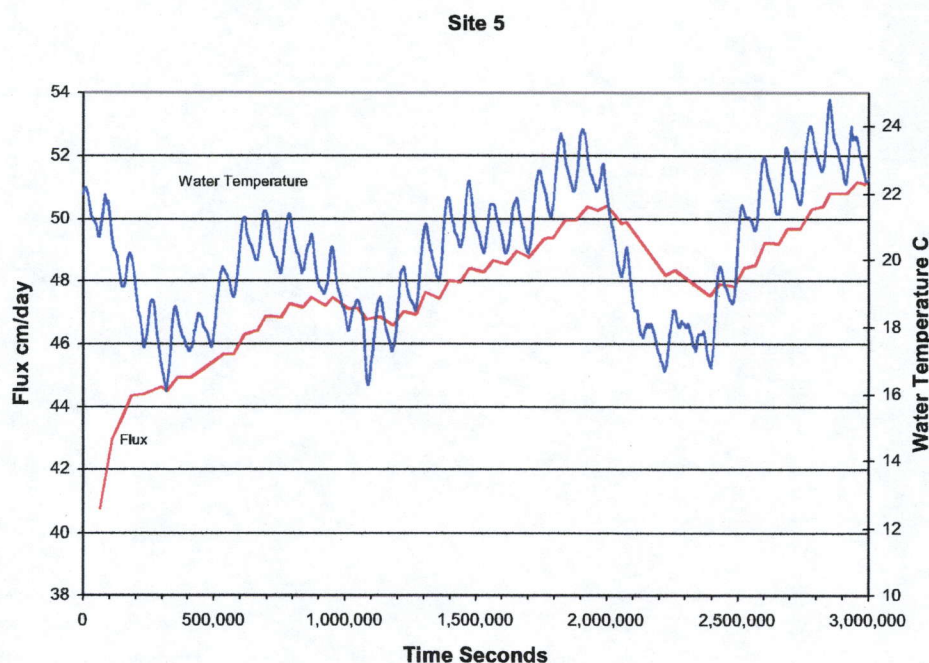
Site 5

Figure 34.   Water temperature and flux rate at Site 5 for the modeled time period.

Site 6

Site 6 is the easternmost monitoring site for this project and is located 457 m east of the eastern end of the geophysical survey. Near Site 6 where the geophysical survey was conducted the data indicated that the area had a moderate saturation potential, which persisted for 2,225 m. (See Figure 1). The sensor arrays at Site6 consist of 4 sensors driven below the canal, three sensors installed in the angled borehole beneath the canal and three sensors installed in the vertical borehole adjacent to the canal (See Figure 35).

Site 6 Model

The model domain for Site 6 was set up with a 62 by 78 cell matrix. Temperature data used in the simulation are from a 35-day time period May 31 to July 5, 2001. Figures 36 to 39 show the comparison of the measured temperatures to simulated temperatures for the sensors beneath the canal at Site 6. TCN 6-8, TCN 6-7 and TCN 6-6 show very good agreement between measured and simulated values. The measured values at TCN 6-5 are warmer than the simulated values. Comparing the temperatures in TCN 6-6 and TCN 6-5 indicates that the temperatures are very similar, which would suggest that sensor 5 slipped up the broomstick during installation. Figure 40 shows the measured and simulated temperatures of sensor TCN 6-4, the highest sensor in the angled borehole beneath the canal. Although the variation of simulated temperature values doesn't closely match the variation of measured values, the general trend of the simulated values is correct and the difference in temperature is not significant. The horizontal hydraulic conductivity was estimated by the model to be 2.3×10^{-6} m/s and the anisotropy 0.22. The average flux for the duration of the simulation was estimated to be 7.7 cm/day. Figure 41 shows the estimated flux rate and measured water temperature for the duration of the model run.

23
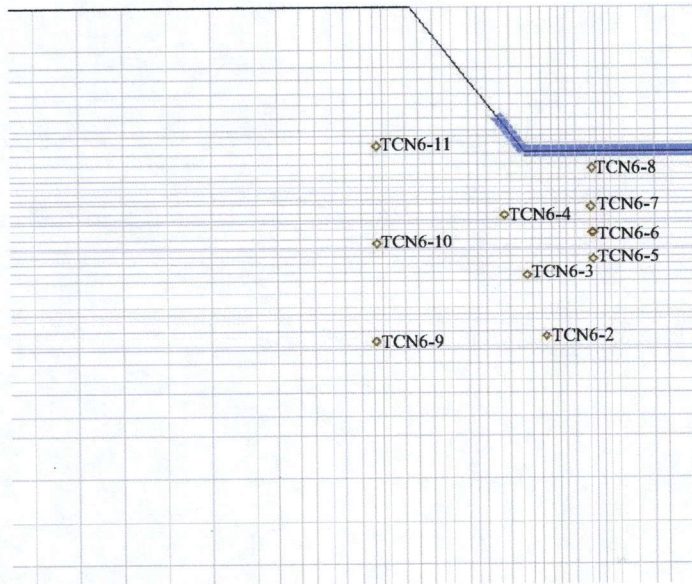
Figure 35. Location of thermocouples and model grid at Site 6.
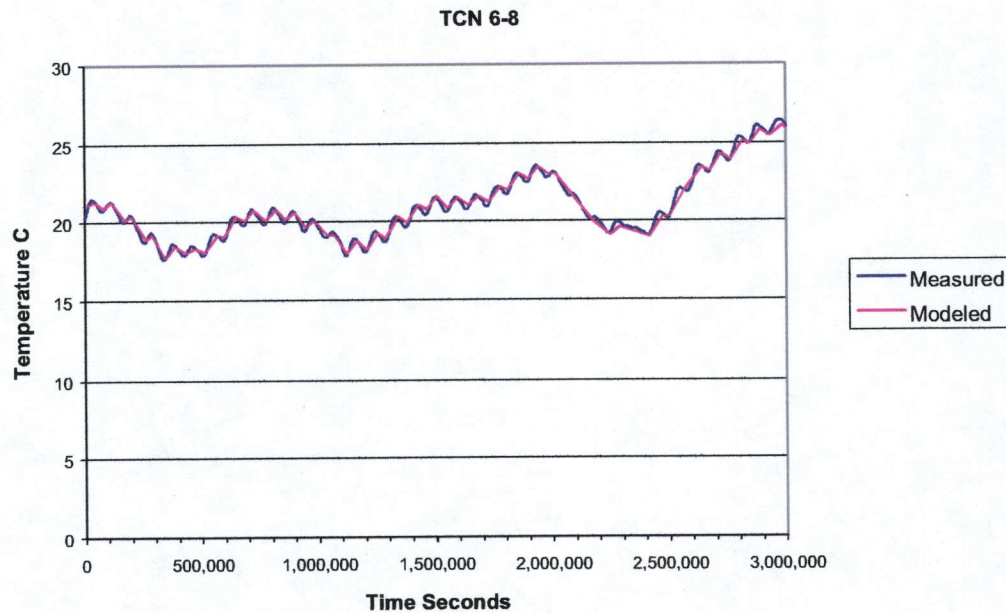
Figure 36. Measured and simulated temperatures for TCN 6-8.

24
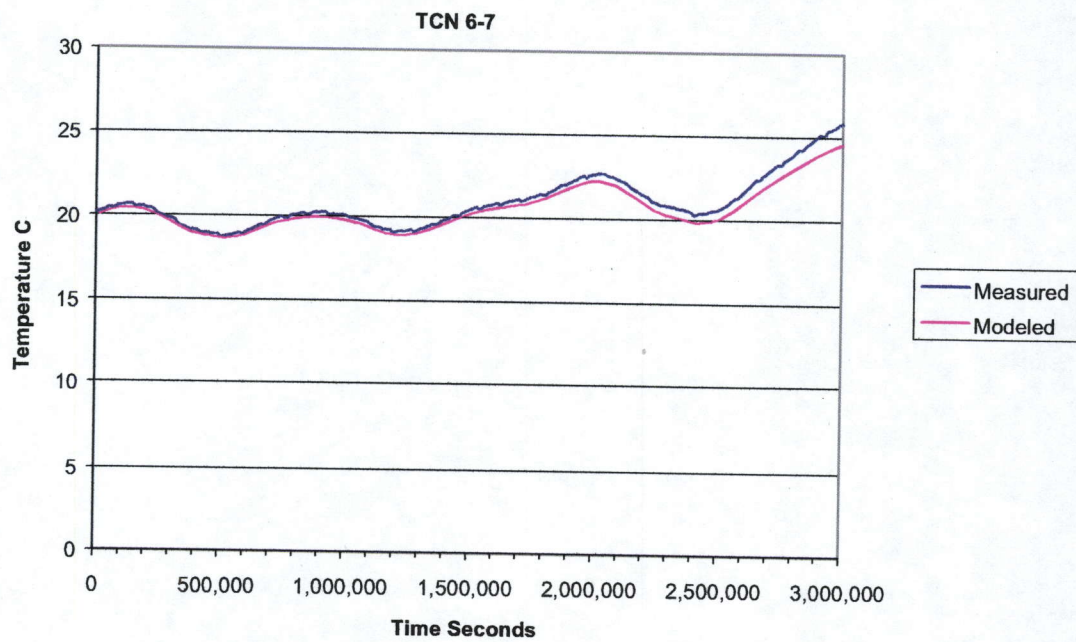
Figure 37.   Measured and simulated temperatures for TCN 6-7.
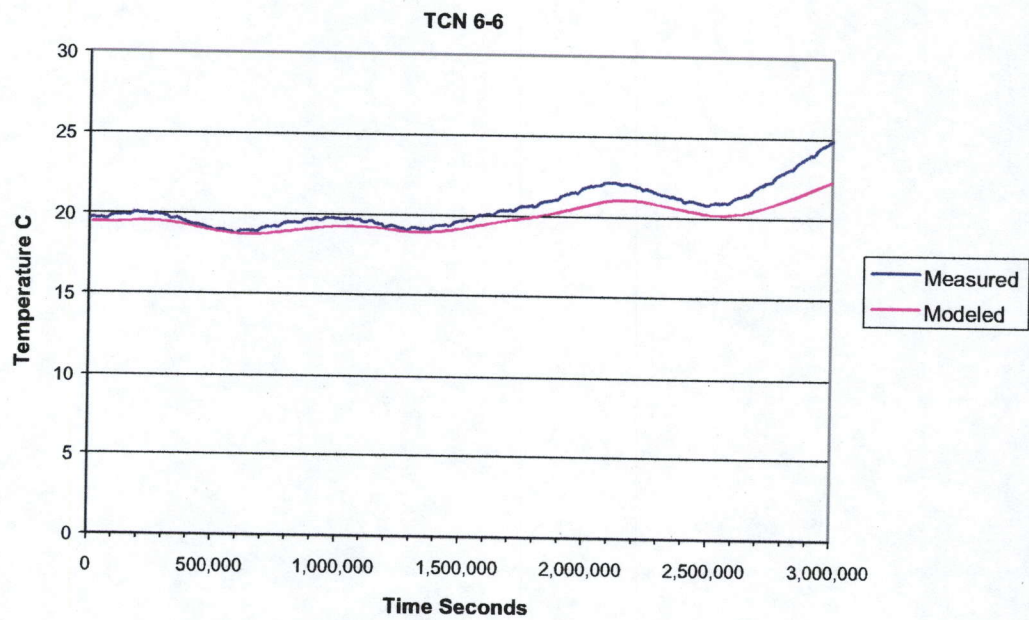
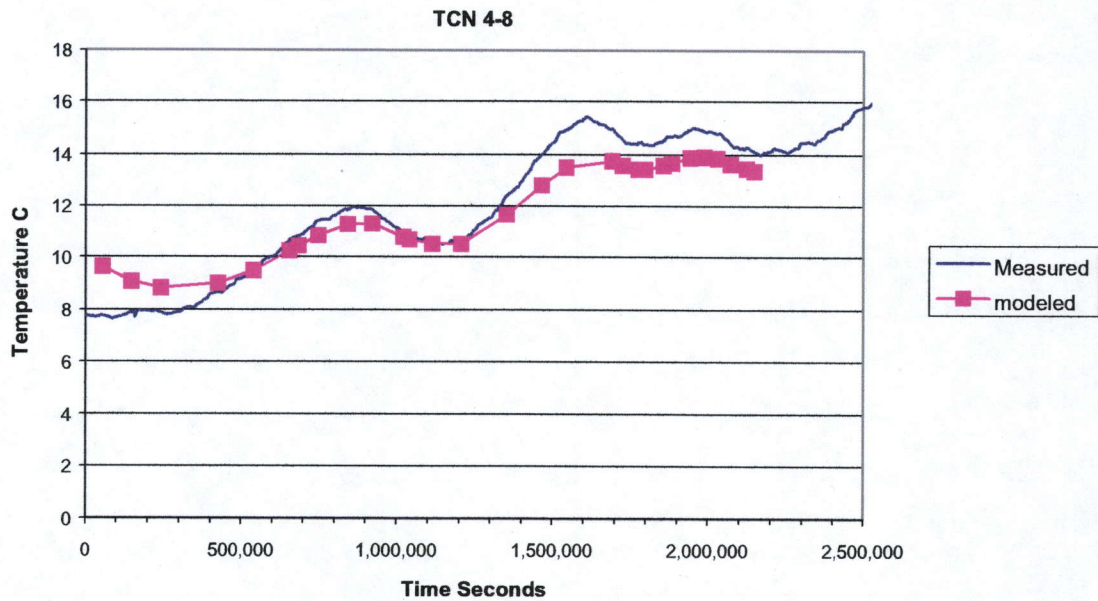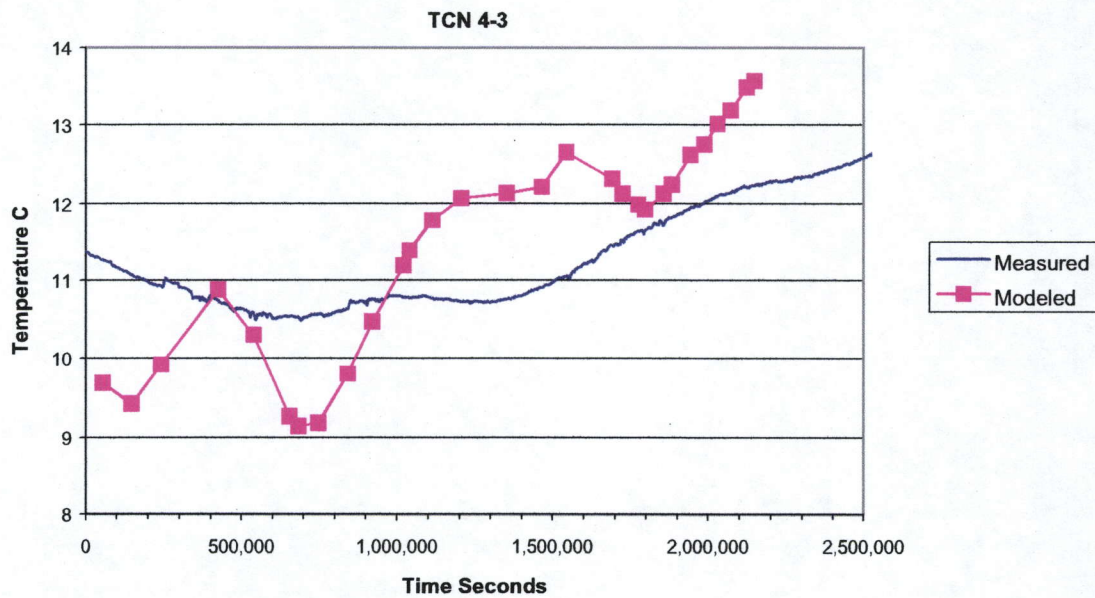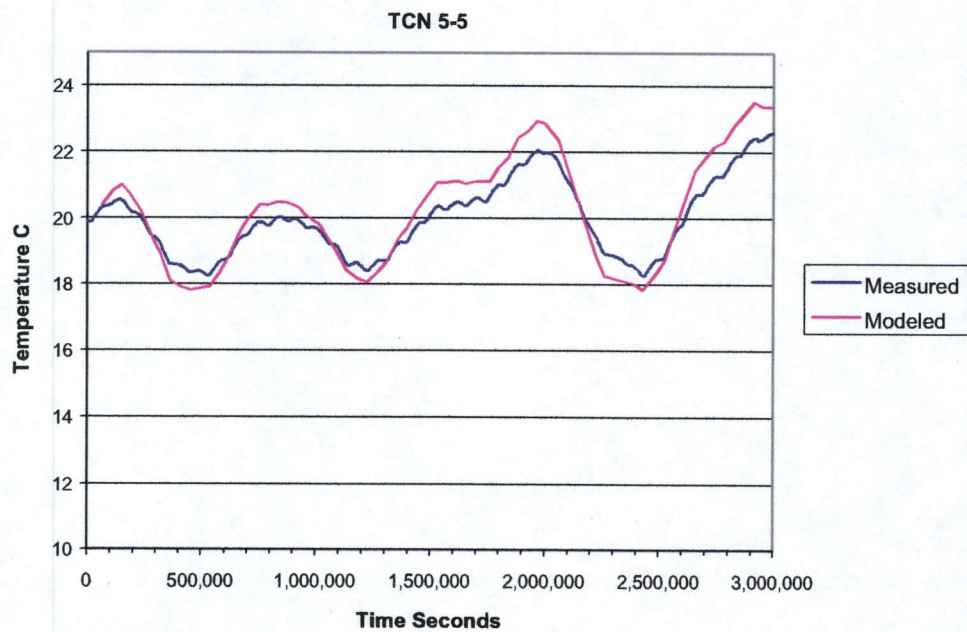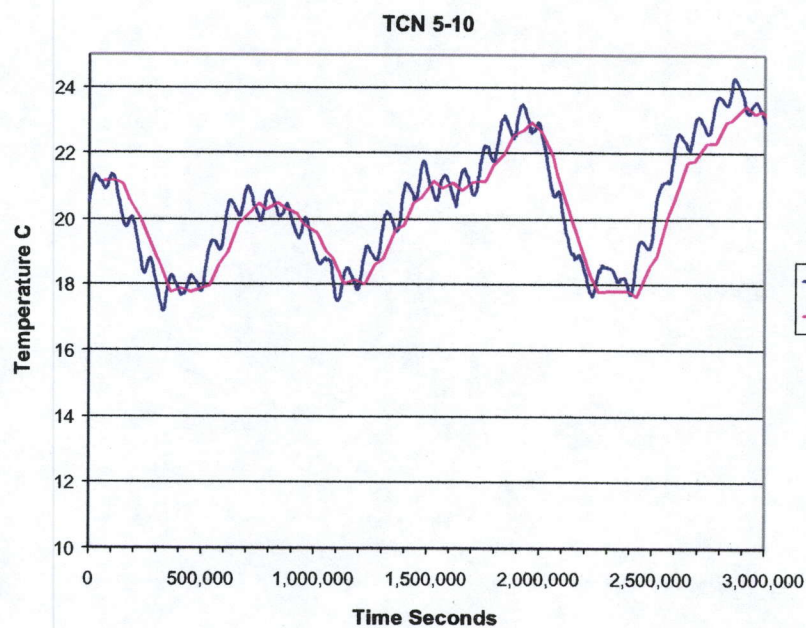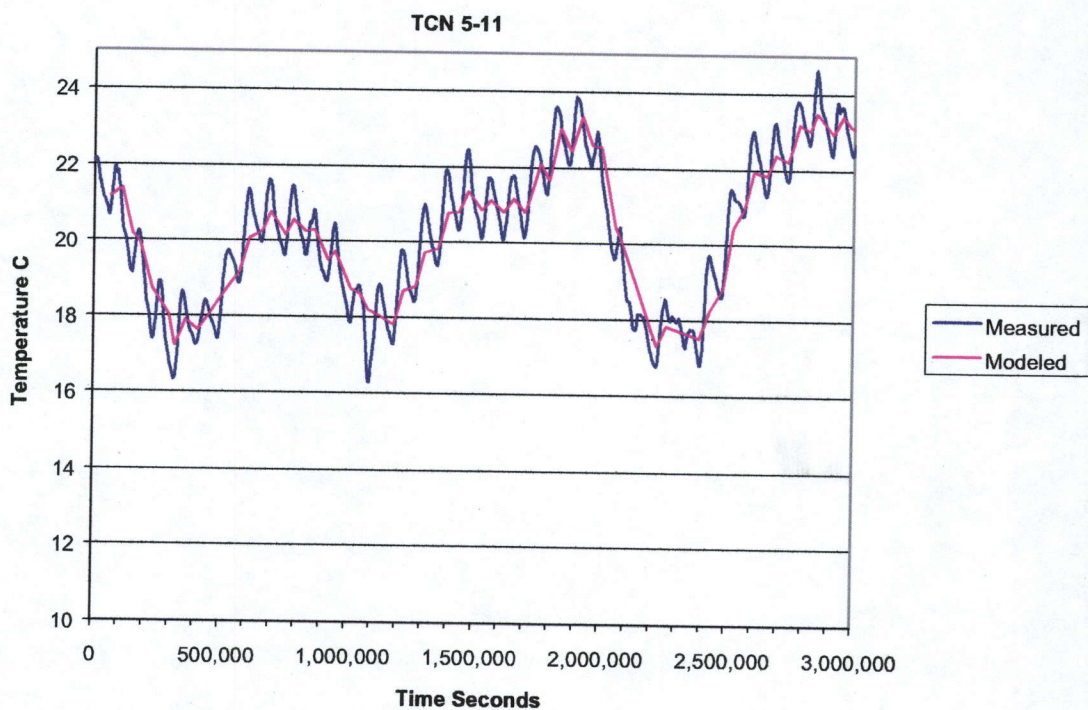Figure 38.   Measured and simulated temperatures for TCN 6-6.

25
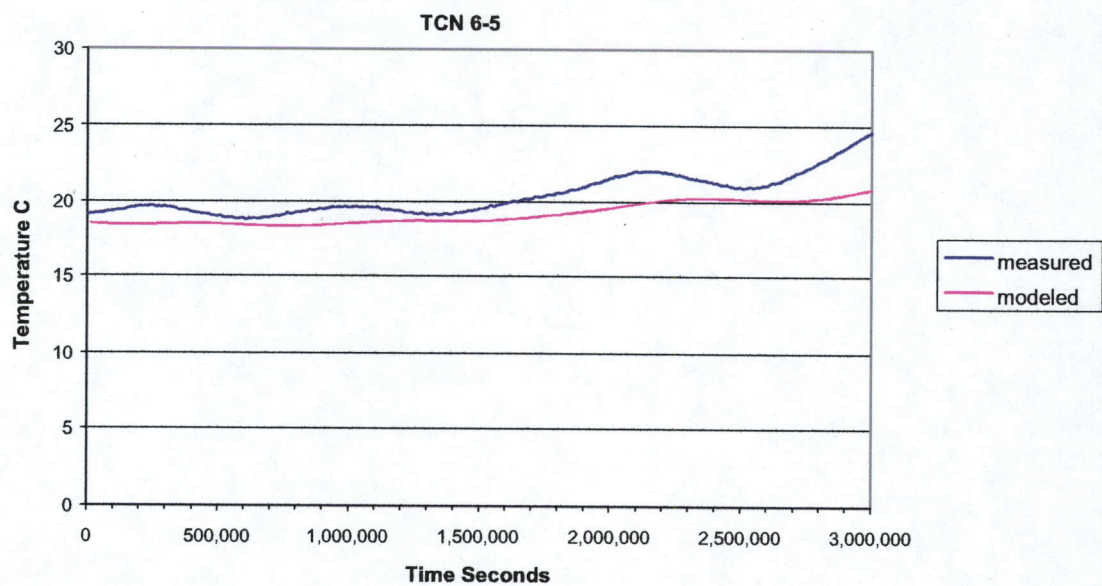
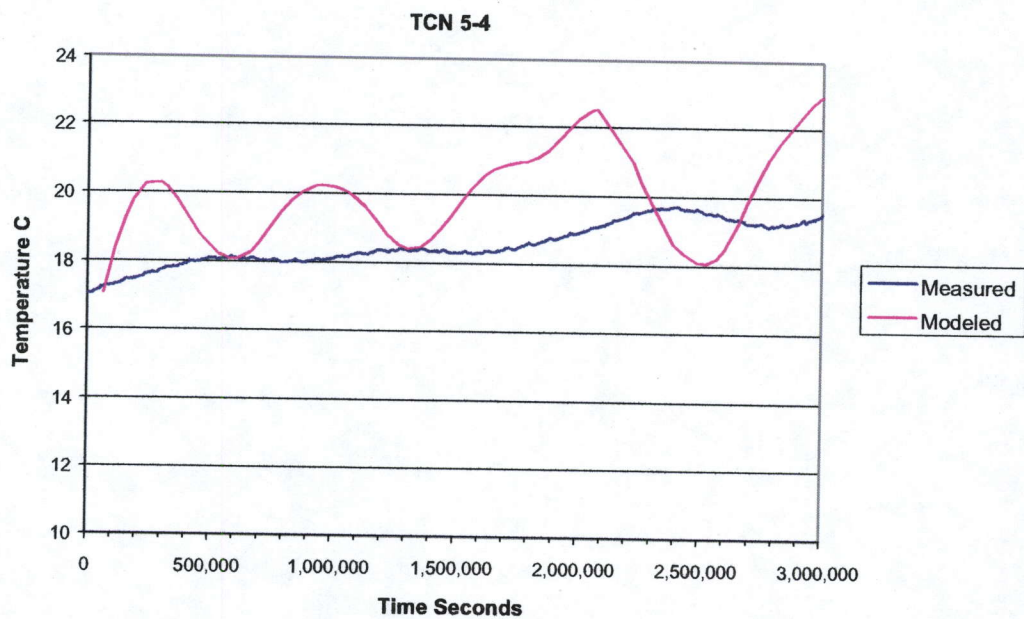Figure 39. Measured and simulated temperatures for TCN 6-5.
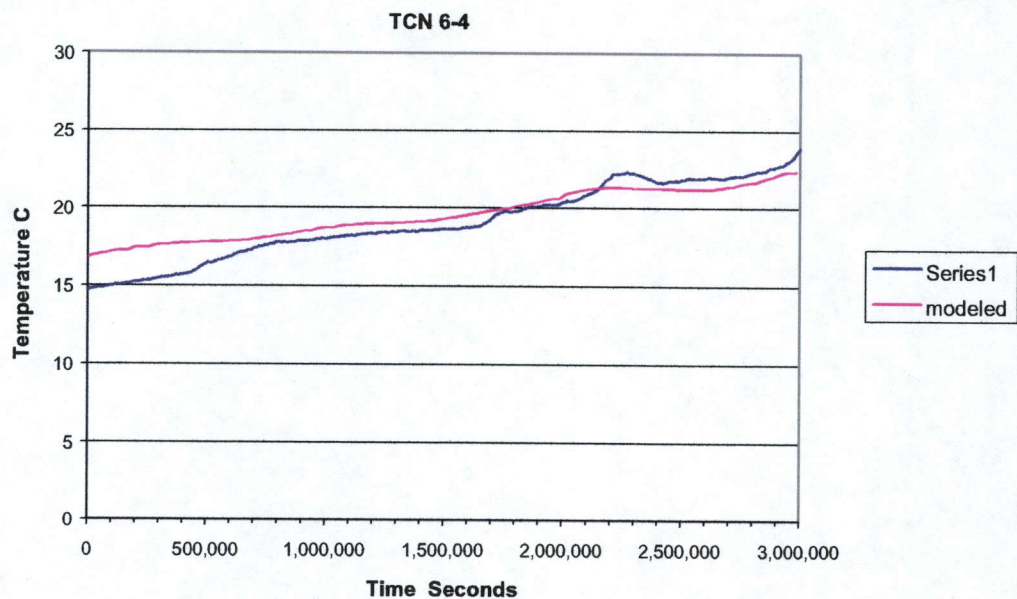
Figure 40. Measured and simulated temperatures for TCN 6-4.
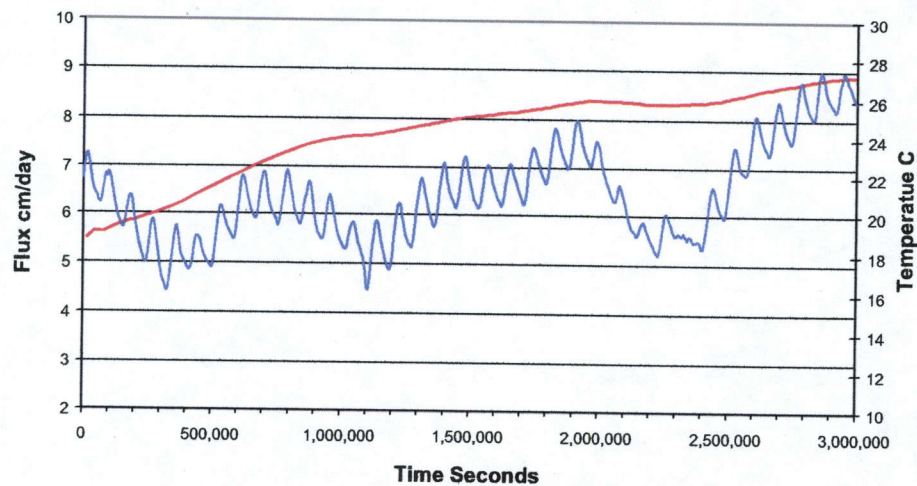
Figure 41.   Water temperature and flux rate at Site 6 for the modeled time period.

LATERAL CANAL PONDING EXPERIMENT/VERIFICATION

A ponding experiment was performed to determine the seepage rate for a representative distribution canal and to verify the use of thermal methods to determine seepage rates. The experiment was located in a distribution canal that is located east of highway 50 (Figure 42). The testing zone consisted of an up-stream gate that was closed to the Truckee canal and a downstream dam constructed on a permanently installed weir. A synthetic liner was installed on the weir to increase the capacity of the ponding experiment to operational levels.
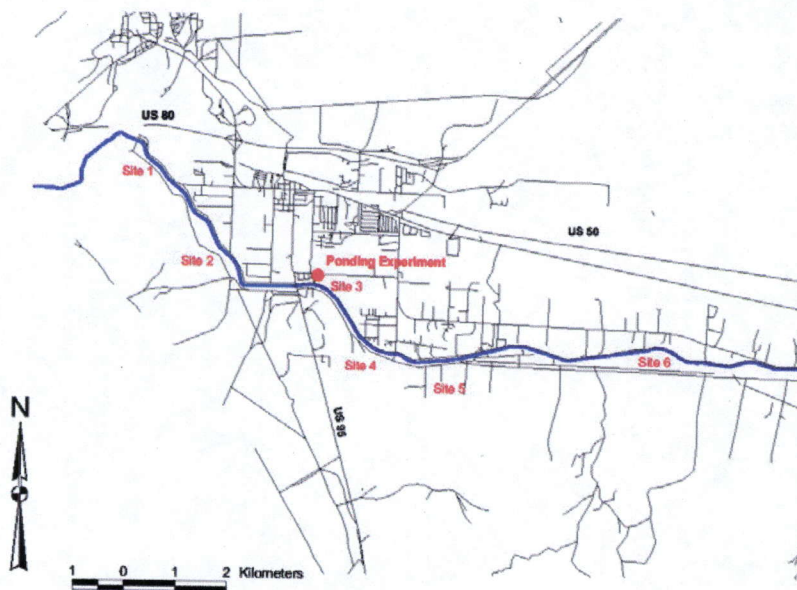
Figure 42.   Location of ponding experiment on a lateral near the Truckee Canal.

Numerous instruments were installed to monitor pond stage, temperature, volumetric water content and matrix potential. A piezometer nest was installed at the edge of the canal, but the water table was found to be well below (30 m) the bottom of the canal, so head measurements could not be made. A Class A evaporation pan was installed approximately 1 m above water surface to determine any losses due to evaporation. Figure 43 shows the location of the pond and surface locations of the instrumentation. Figure 44 shows location of the instrumentation along section A-A'.

Downstream Dam/Weir

Scale

5   10 m

Legend

■   Thermocouple Nest

▲   Data Logger

●   Time Domain Reflectometry
    & Heat Disipation Unit

◉   Piezometer Nest
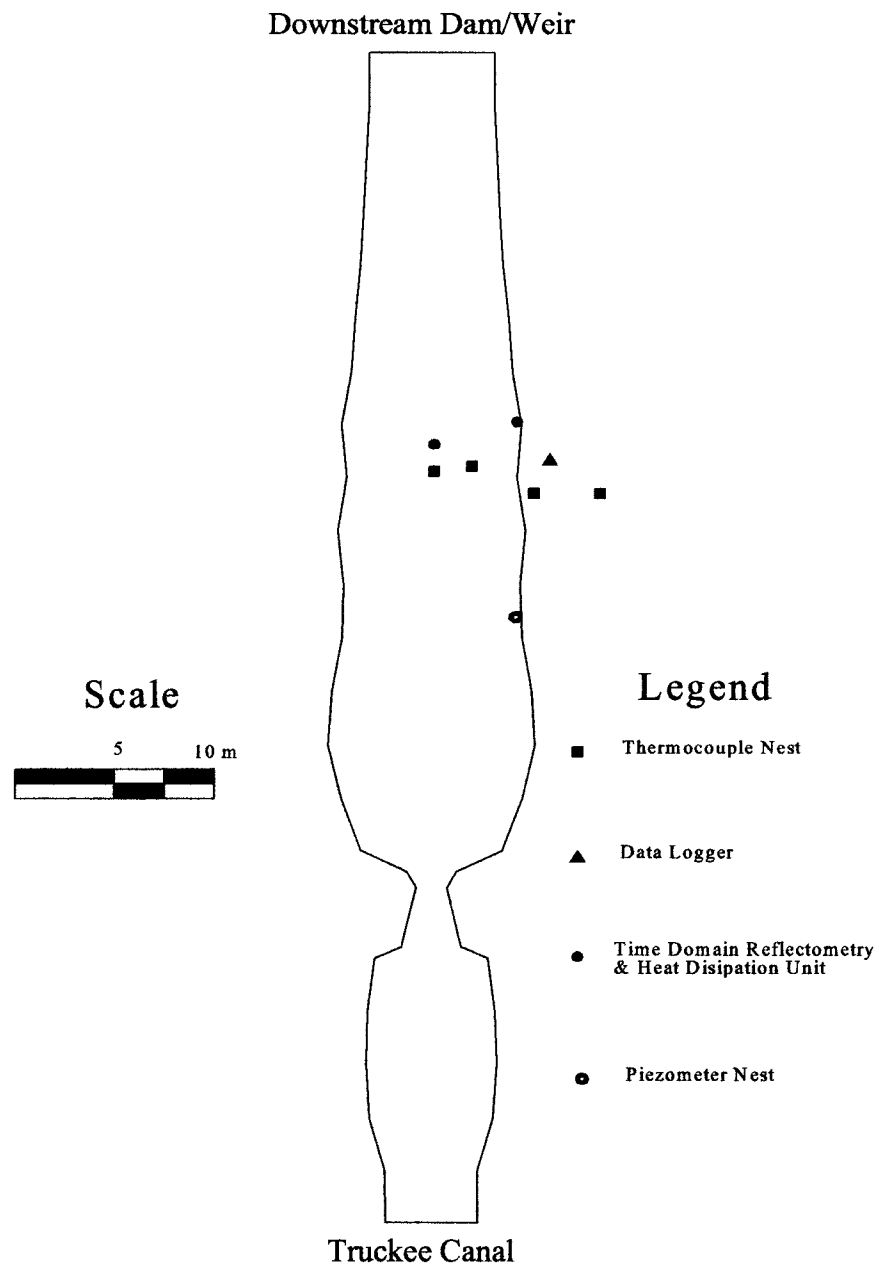
Truckee Canal

Figure 43.   Ponding experiment layout and location of instrumentation.

28

A
TC Nest A'

TC Nest

TC Nest

TC Nest
1-1
1-2
1-3
1-4
1-5

2-1
2-2
2-3
2-3
2-4
2-5

TC Nest
3-1
3-2
3-3
3-4
3-5

TC Nest
4-1
4-2
4-3
4-4
4-5

Legend

■ Thermocouple

□ Heat disipation and TDR

● Heat disipation only
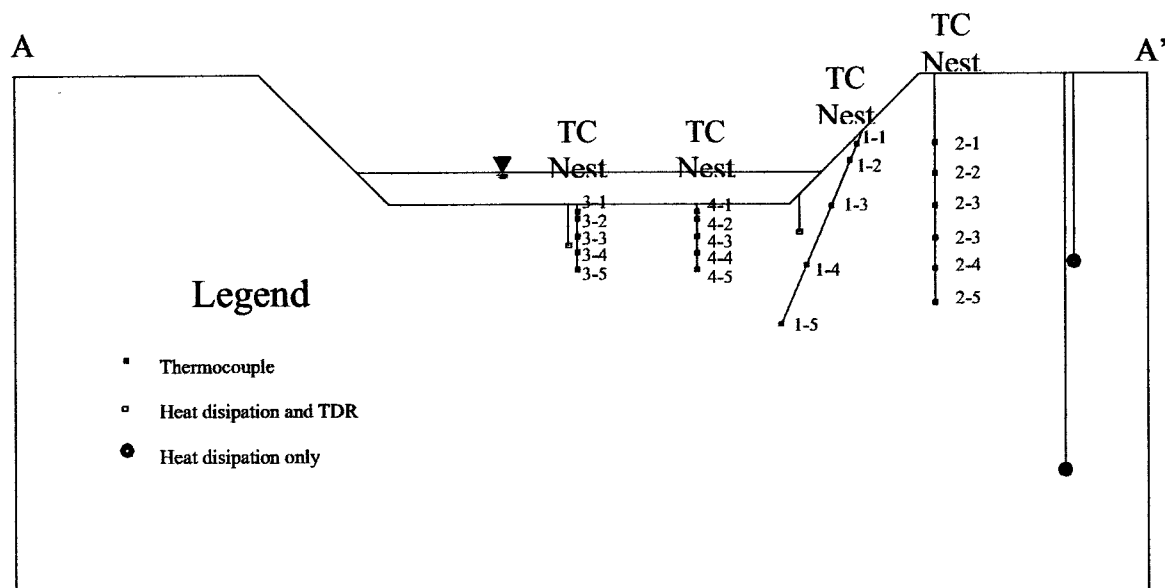
Figure 44. Location of subsurface instruments along section A-A'.

A high-capacity pump was used to withdrawal fluid from the Truckee Canal into the ponded section. A flowmeter was installed inline to measure the volume of fluid discharged. The pond was essentially empty prior to the experiment, but water contents were elevated due to standing water through the winter. Pumping was initiated on March 21, 2001 at 16:37. The entire experiment continued through March 27, 2001 at 14:45. Although data were collected during this period, the data from the first two days were not used in the analysis to allow the seepage to come into equilibrium.

Thermocouple, matrix potential, and water content data were collected digitally at 15 min-increments. The evaporation pan was filled on a daily basis to determine evaporative losses. Stage was measured on a daily basis and fluid was added to return the stage to 0.61 m (2.0 ft) above the bottom of the pond. Again, the volume of fluid discharge was recorded.

Table 1 shows evaporation rates, seepage rates, discharge volumes, and staff gauge readings during the ponding experiment. The seepage flux was calculated using the change in the staff gauge measurements and also using the fluid volume required to refill the pond. The volume method utilized a surface area of 477 m^2 as determined by the site survey. The seepage rates are relatively large at the beginning of the experiment and then quickly decrease to a quasi-equilibrium state. This type of infiltration behavior is expected, as the initially dry soils have a larger infiltration capacity. As the water content increases beneath the pond, the infiltration rate stabilizes.

A coupled flow and thermal transport model was used to validate the use of thermal measurements to determine seepage rates. FEFLOW (Diersch, 1998) was chosen as the numerical simulator due its ability to handle complex boundary conditions (varying stage) with ease.

Table 1.   Results of the ponding experiment including seepage loss, evaporation, discharge volumes and times, and staff gauge readings.

Date	Pump Start Time	Discharge Volume (m³)	Evaporation Rate (m/day)	Volumetric Seepage Loss (m/day)	Staff Gauge Seepage Loss (m/day)	Staff Gauge Initial Level (m)	Staff Gauge Final Level (m)
3/21/01	16:37	----	----	----		0.000	0.750
3/21/01	18:49	2178	----	0.415	0.439	0.722	0.750
3/22/01	8:12	2238	2.65E-03	0.204	0.202	0.594	0.719
3/22/01	15:05	2244	2.80E-02	0.053	0.056	0.661	0.674
3/23/01	9:12	2267	2.79E-03	0.060	0.062	0.561	0.610
3/24/01	8:36	2323	3.04E-03	0.114	0.121	0.494	0.616
3/25/01	19:33	2380	3.51E-03	0.081	0.086	0.488	0.613
3/26/01	14:07	2412	4.23E-03	0.089	0.085	0.546	0.610
3/27/01	14:45	2464	5.63E-03	0.099	0.108	0.497	0.610

Although the thermal model is transient in flow and thermal transport, the period of simulation was chosen after the initial equilibrium period to ensure that all of the instrumentation had stabilized and was operating properly. The period of simulation began on March 24, 2001 at 0:00 hrs and continued through March 27, 2001 at 14:38 hrs.

The hydraulic and thermal boundary conditions are shown in Figures 45 and 46, respectively, along with the finite element grid used to subdivide the model domain. Hydraulic boundaries consist of no-flow vertical boundaries representing the axis of symmetry and the vertical boundary outside of the canal section. The lower boundary is simulated with a pressure head of zero to represent the water table conditions. The upper boundary varies between a temporally varying specified head to represent the time-varying pond stage (see Figure 47) and no-flow conditions above the fluid level in the canal. The thermal boundaries are represented by no energy flow along both vertical boundaries. The lower boundary is represented as a constant temperature of 14°C to represent the relatively constant temperature at this depth. The upper boundary is represented by a temporally varying specified temperature condition for the fluid temperature (Figure 48) and the soil temperature (Figure 49).

Numerous thermal and hydraulic parameters are required to construct the model. The soil retention parameters (van Genuchten alpha, and n), porosity, are chosen based on soil texture (Carsel and Parrish, 1988). The thermal parameters such as the heat capacity, thermal conductivity, and thermal dispersivity are taken from Jury et al., 1991. All of these parameters are relatively well known and are shown in Table 2. The saturated hydraulic conductivities in the vertical and horizontal directions are assumed to be unknown parameters and determined via a trial-and-error calibration procedure.

Table 2.   Thermal parameters used in FeFlow (after Jury et al., 1991).

van Genuchten Retention Parameters		Porosity	Heat Capacity		Thermal Conductivity		Thermal Dispersivity	
Alpha (1/m)	n ()	()	Dry Soil (J/m³/C)	Fluid	Dry Soil (J/m/s/C)	Fluid	Longitudinal (m)	Transverse
12	1.96	0.4	2.00E+06	4.20E+06	0.3	1	1	0.1

Legend

━━━ No-Flow

━━━ Specified Head

31.75, 25

-8,, 22.6

-8,-8

31.75,-8
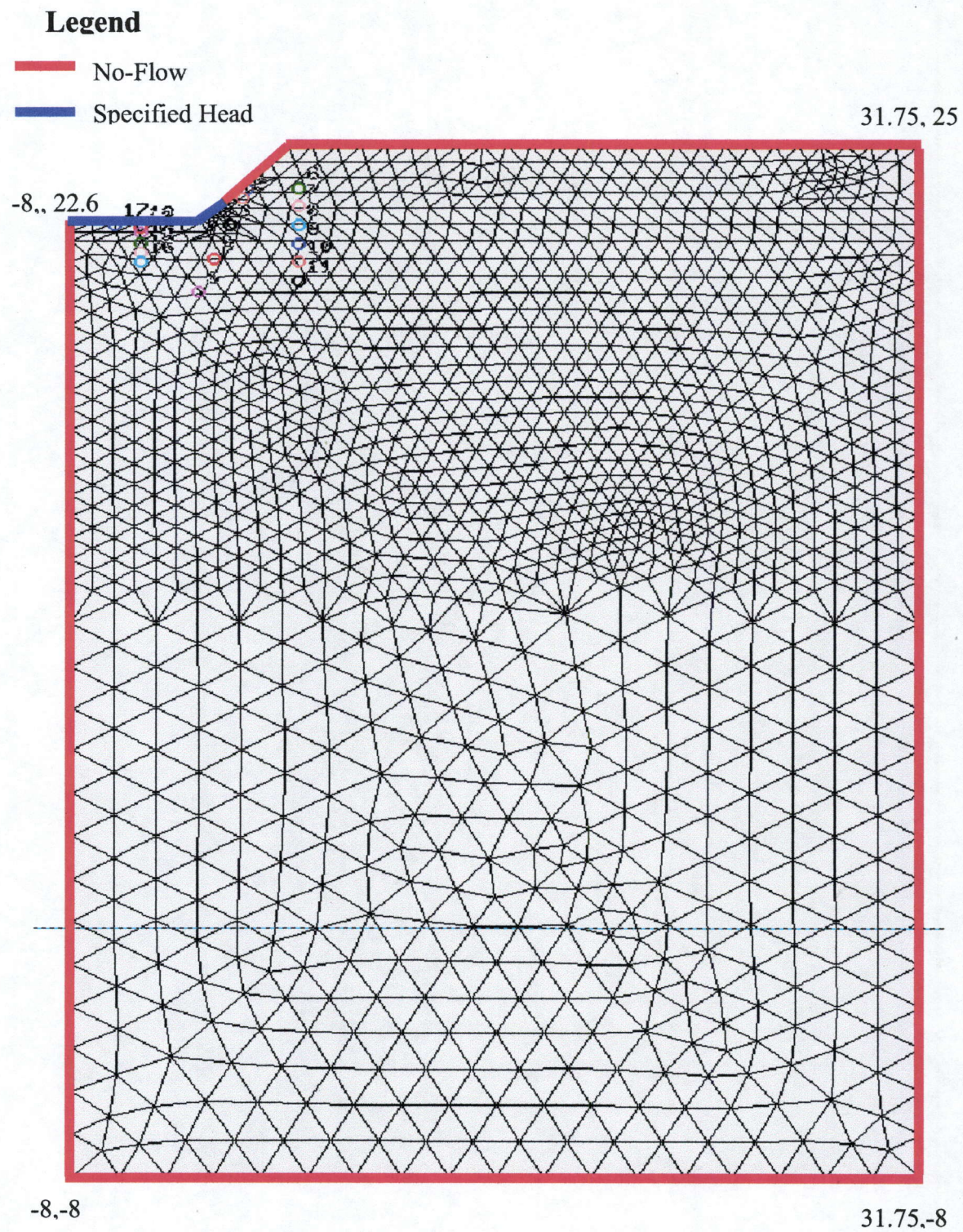
Figure 45. Hydraulic boundary conditions and finite element grid for the lateral flow and thermal model.

31

Legend

- ▬ No Energy Flow
- ▬ Specified Temperature (Constant at 14°)
- ▬ Specified Temperature (Temporally varying water temperature)
- ▬ Specified Temperature (Temporally varying air/soil termperature)
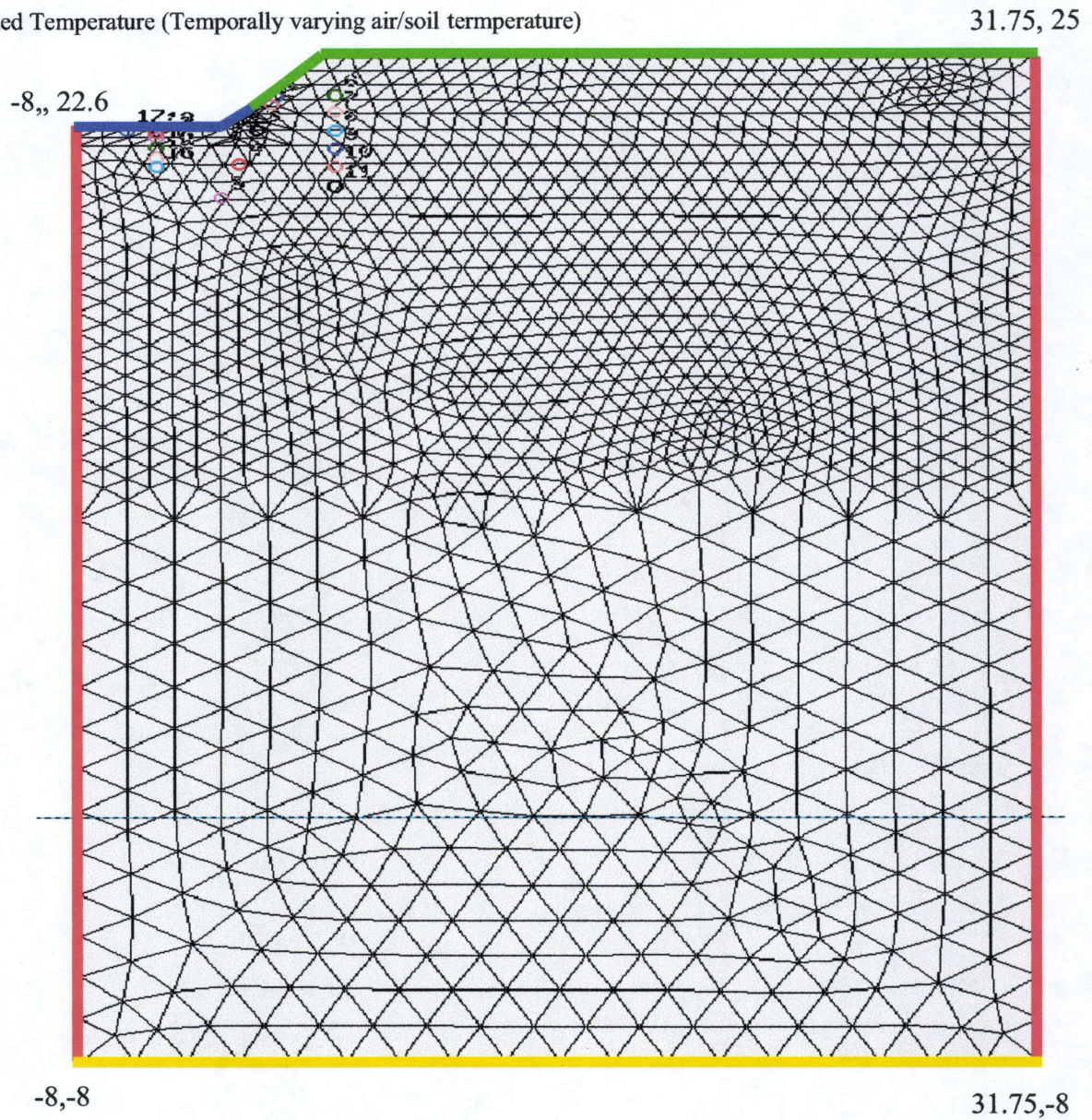
31.75, 25

-8,, 22.6

17:3

-8,-8

31.75,-8

Figure 46. Thermal boundary conditions and finite element grid for the lateral flow and thermal model.
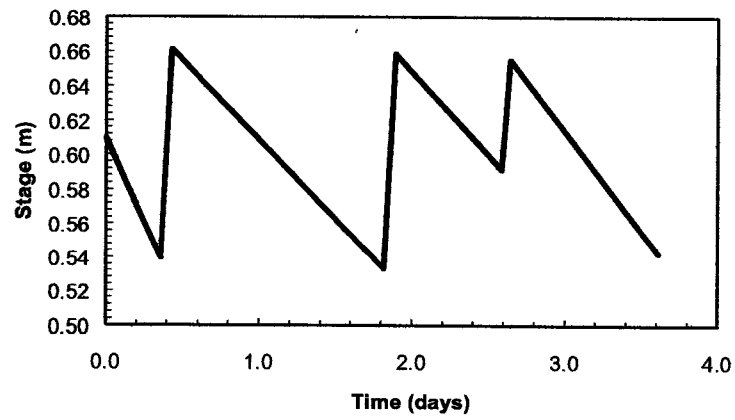
Figure 47. Varying pond stage used in simulation.
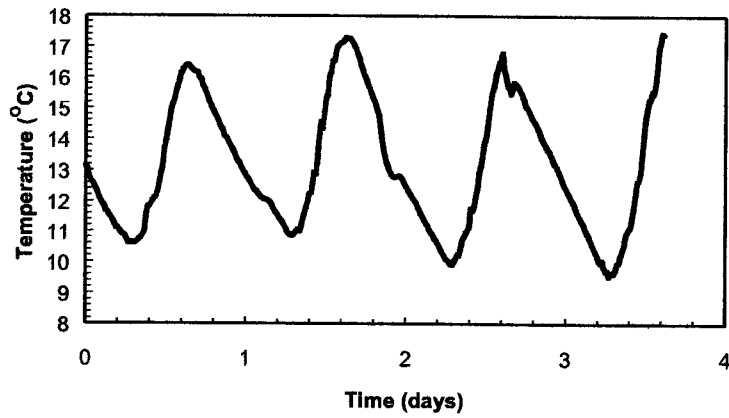

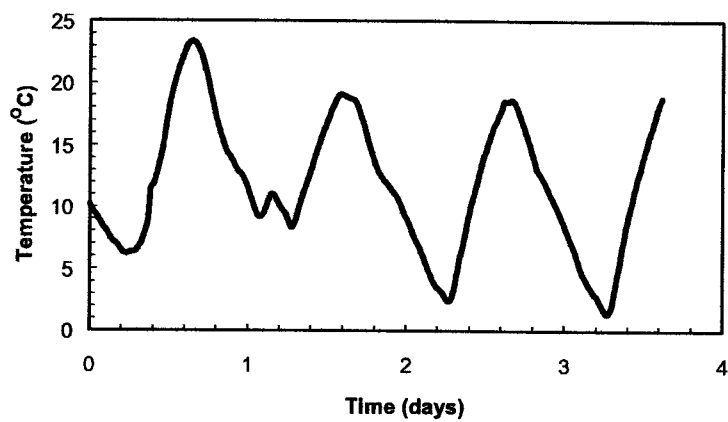Figure 48. Water temperatures used for simulation at the ponding experiment.

Figure 49. Soil temperature used for simulations at the ponding experiment.

33

The thermal and hydraulic initial conditions were generated from the thermocouple nests and TDR probes, respectively. The temperature profile at the beginning of the simulation was generated via standard kriging interpolation techniques (Deutsch and Journel, 1992) such that observation data could be mapped to grid nodes. An initial volumetric water content of 0.25 was applied to the entire model domain as determined from the TDR probes.

The calibration procedure consisted of adjusting the vertical and horizontal hydraulic conductivities until there was a general agreement between the observed and simulated temperatures during the 3.61-day simulation period. A smoothing procedure was employed to reduce the noise in the temperature data to reduce the impact of electronic noise on the calibration procedure.

The results of the simulated versus observed temperatures are shown in Figures 50 to 52 for thermocouple nest 1, 2, and 4, respectively. Thermocouple nest 3, was used as a replicate and showed similar results to nest 4, so these data were not used explicitly in the calibration procedure. In general, there is a good agreement between the observed and simulated temperatures throughout the simulation period. Thermocouple nest 1, which is installed at an angle from the pond bank to a zone beneath the pond, shows a gradually increasing trend in both observed and simulated values. The slightly elevated temperatures in the simulated temperatures are due to the interpolation method required to process the initial temperatures from the observation points to the grid nodes. A similar pattern is seen in thermocouple nest #2, which is located adjacent to the ponded zone. Both thermocouple nests 1 and 2 exhibit only small changes in temperature throughout the simulation period, as these zones are not directly impacted by vertical seepage. Simulated temperatures in thermocouple nest 4 are also exhibiting the same general increasing trend, but diel fluctuation is not simulated to the same degree as observed. The data from thermocouple nest 4 were not smoothed as it was felt that the diel trends were larger in amplitude as compared to other nests and as such represented real variability. A certain degree of the variation can be attributed to electronic noise caused by variations in temperature at the datalogger.

Figures 53 to 56 show the simulated temperature profile for 1.0, 2.0, 3.0 and 3.61 days from the start of the simulation for the upper portion of the model domain. In general the majority of the temporal fluctuations are constrained to the near-surface horizon.

The purpose of the ponding experiment was to determine the seepage rates from a representative lateral canal and to verify the efficacy of the thermal methodology. The seepage rates as determined from the thermal model are compared to the independent estimates of seepage as presented above. Figure 57 shows the observed versus simulated seepage rates during the ponding experiment. The observed versus simulated seepage rates are in general agreement with the simulated seepage rates, with the simulated rates being overestimated by approximately 0.01 m/day (1 cm/day). The simulated temperatures underestimate the seepage rates by a maximum of 0.03 m/day (3 cm/day) during the final few hours of the experiment, which is most likely due to a small leak that developed at the downstream dam during the final hours of the experiment.
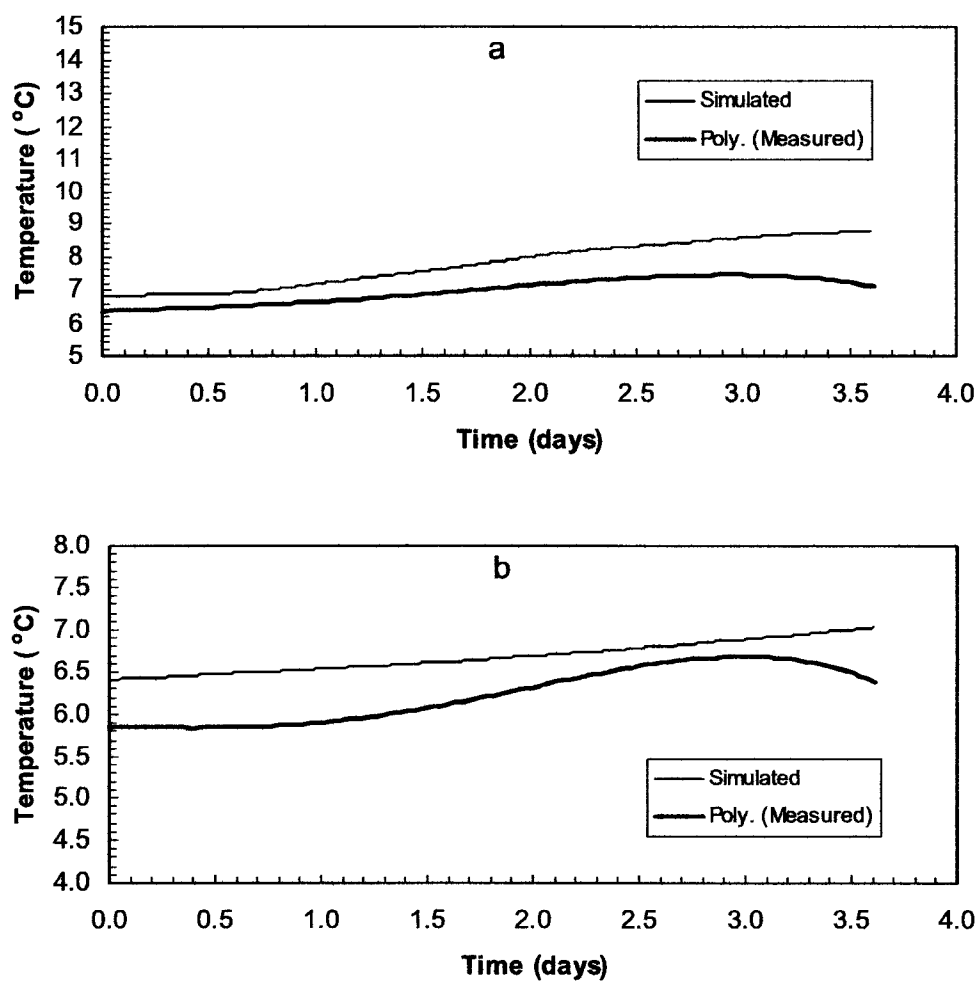
Figure 50. Simulated versus observed temperatures for thermocouple nest # (a) represents thermocouple nest #1-3 (b) represents nest #1-5.
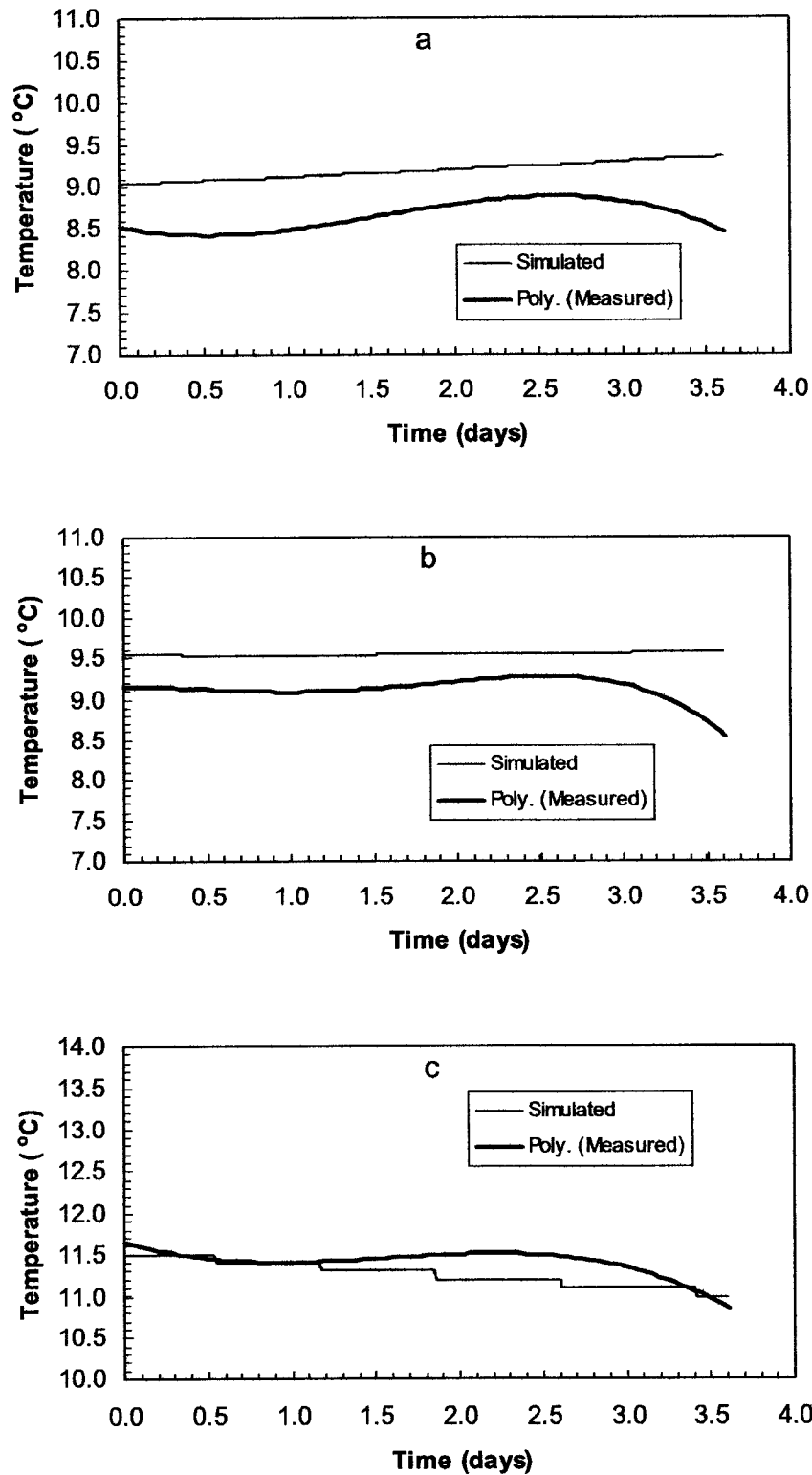
Figure 51. Simulated versus observed temperatures for thermocouple nest #2 (a) represents thermocouple nest #2-1 (b) represents nest #2-3 (c) represents nest #2-6.
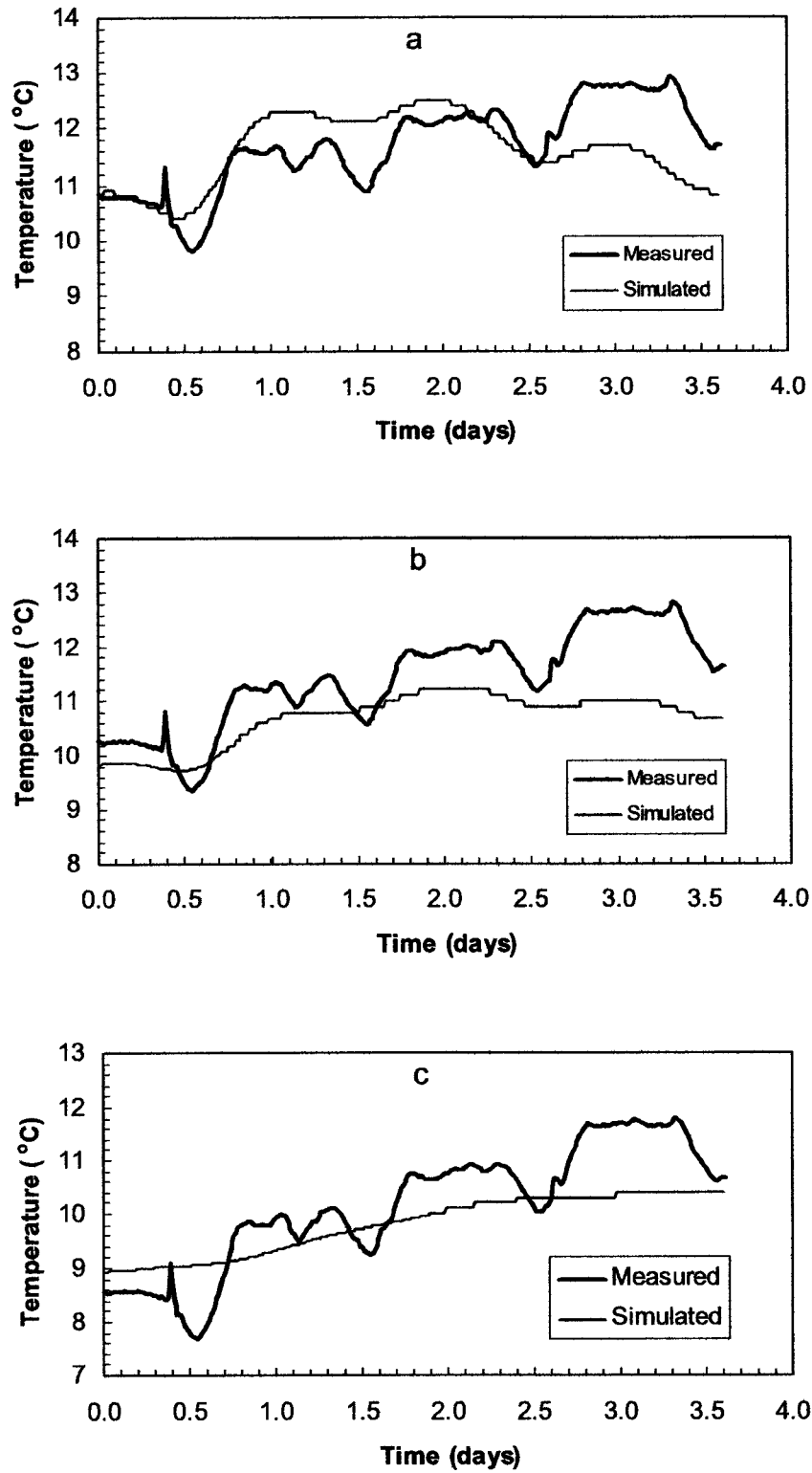
Figure 52. Simulated versus observed temperatures for thermocouple nest #4 (a) represents thermocouple nest #4-3 (b) represents nest #4-4 (c) represents nest #4-5.
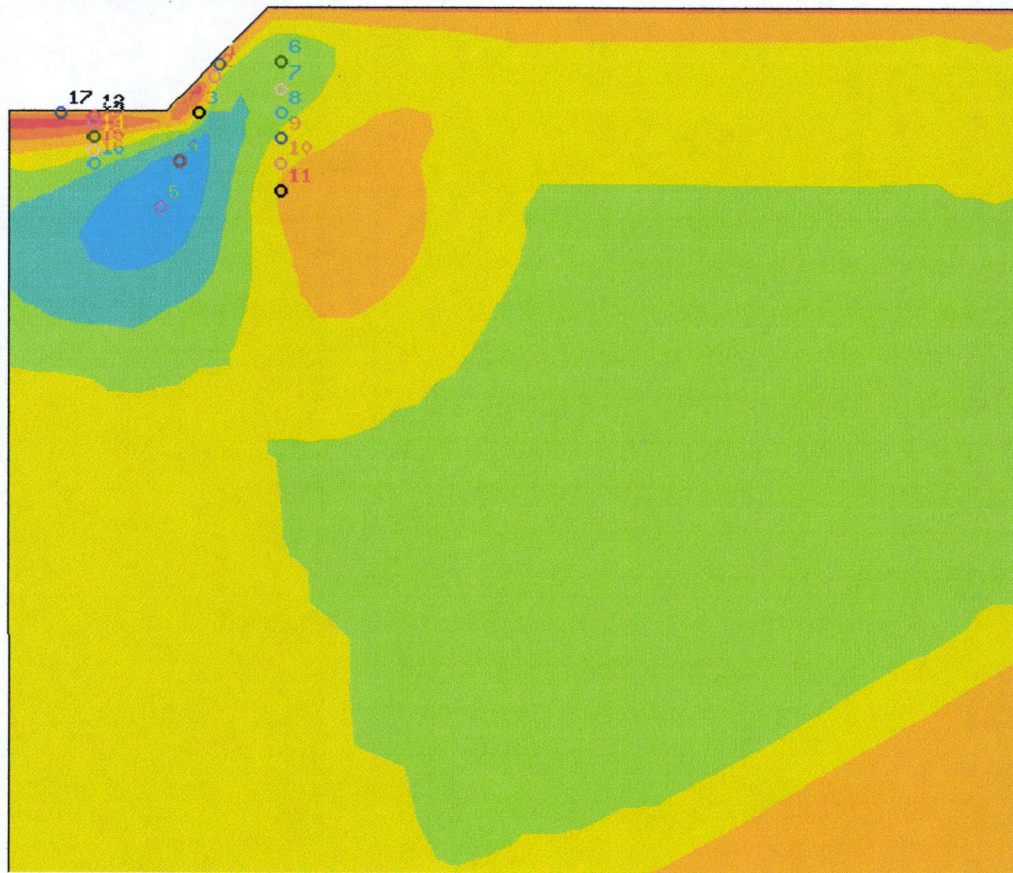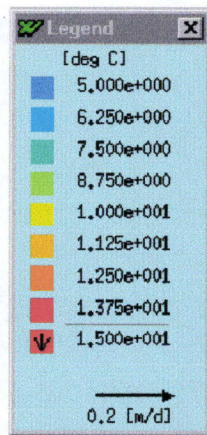
Figure 53.   Simulated temperature profile one day after the start of the simulation.
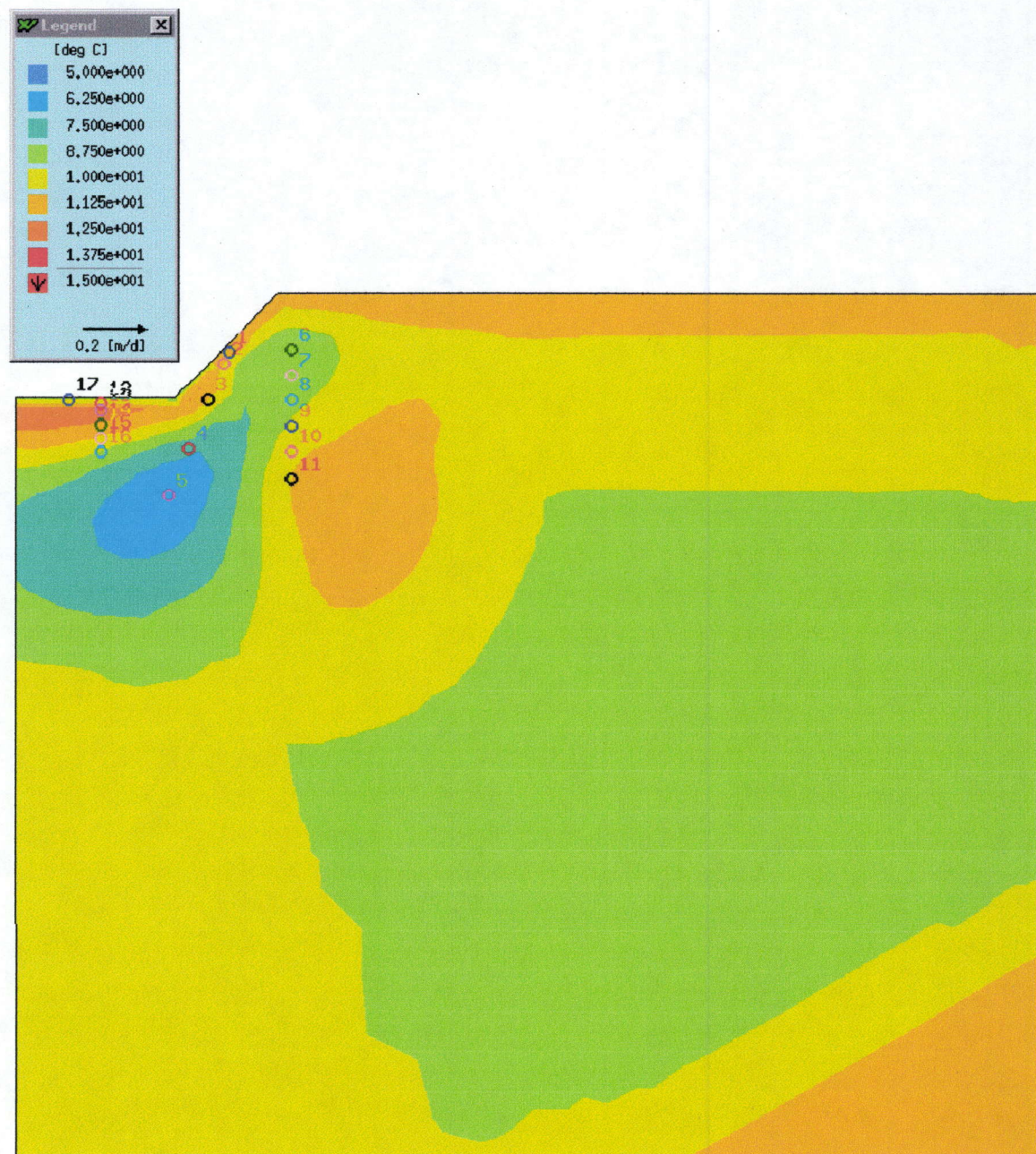
Figure 54.   Simulated temperature profile two days after the start of the simulation.
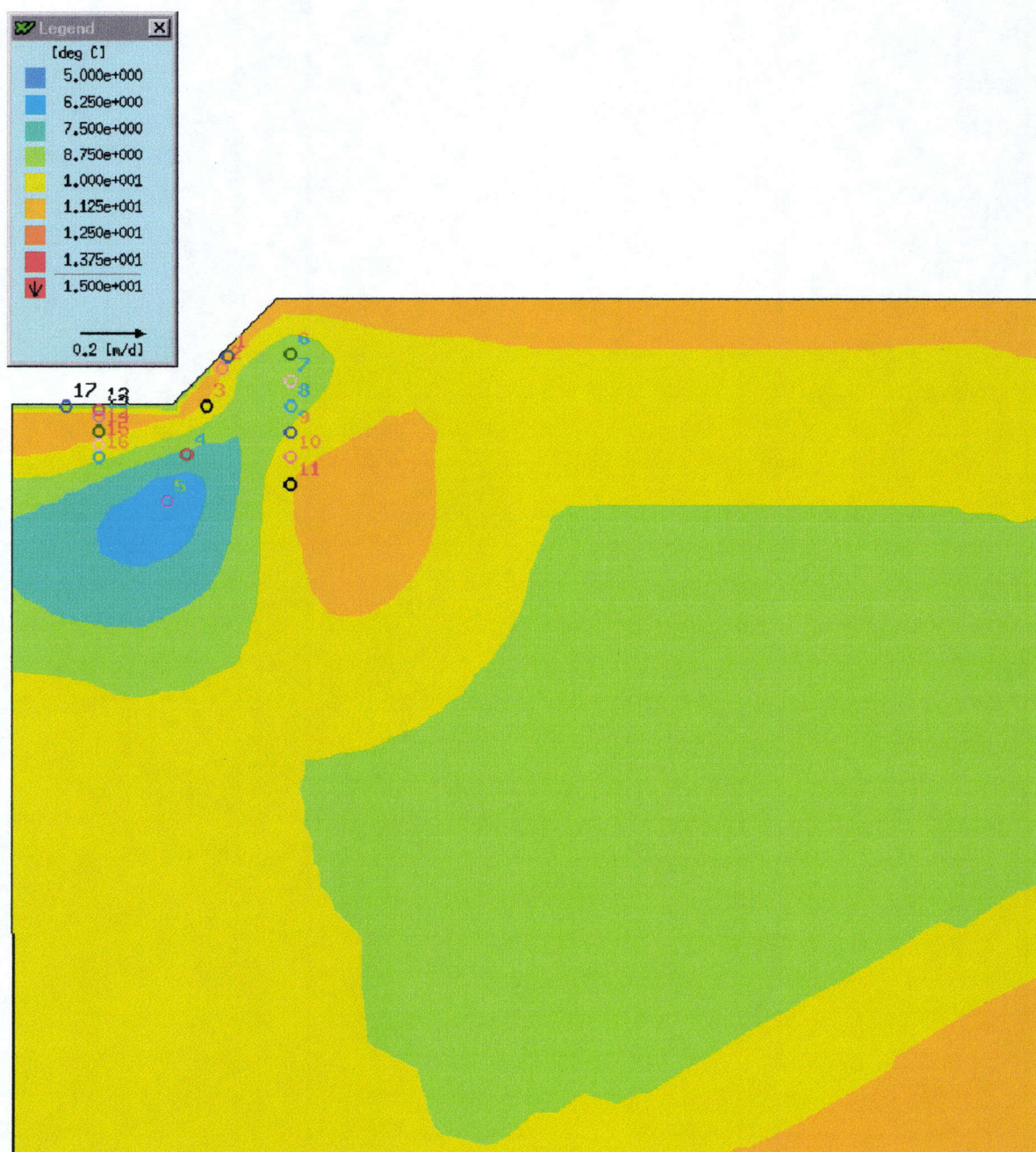
Figure 55.   Simulated temperature profile three days after the start of the simulation.
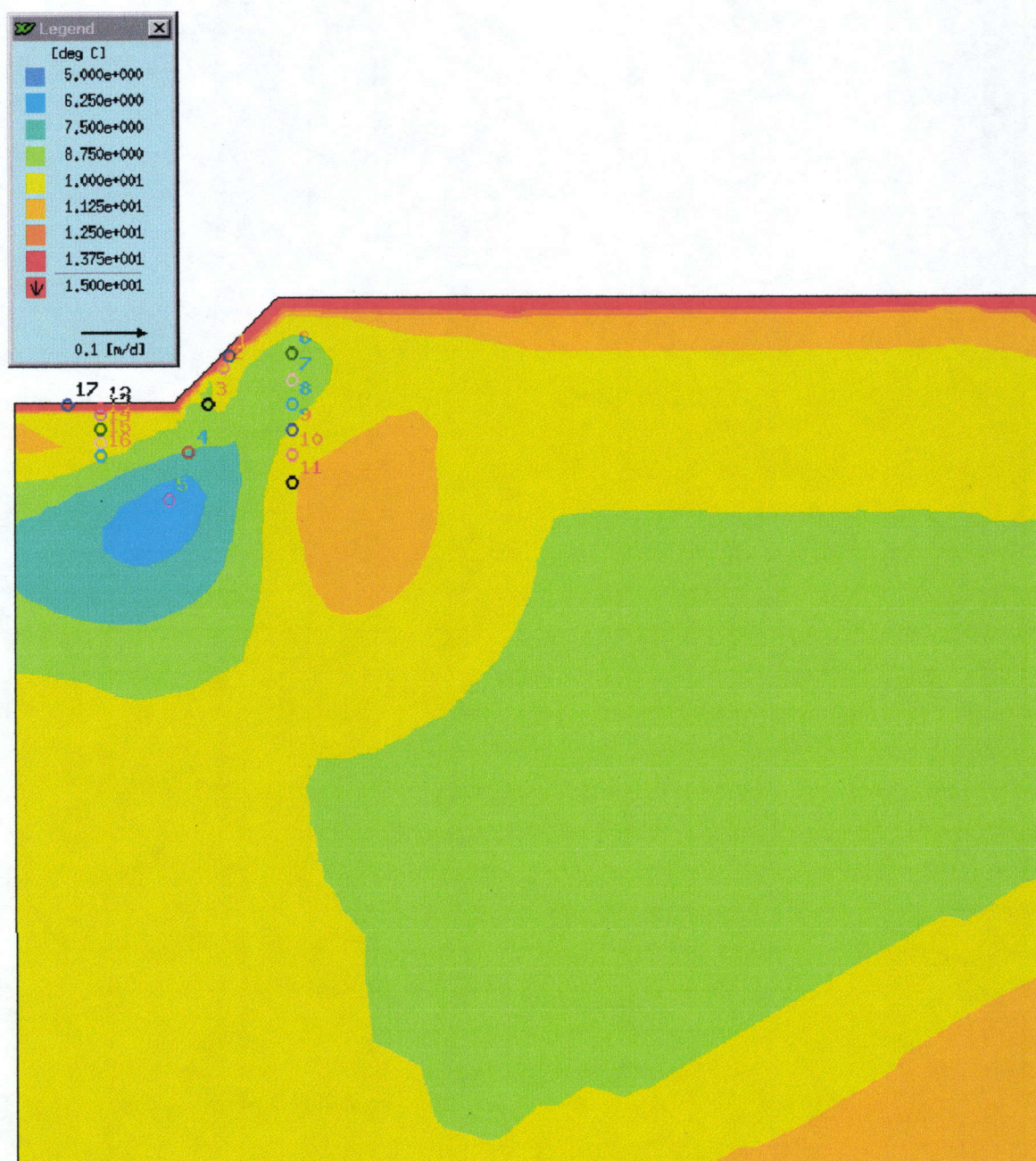
Figure 56. Simulated temperature profile 3.61 days after the start of the simulation (final time step).
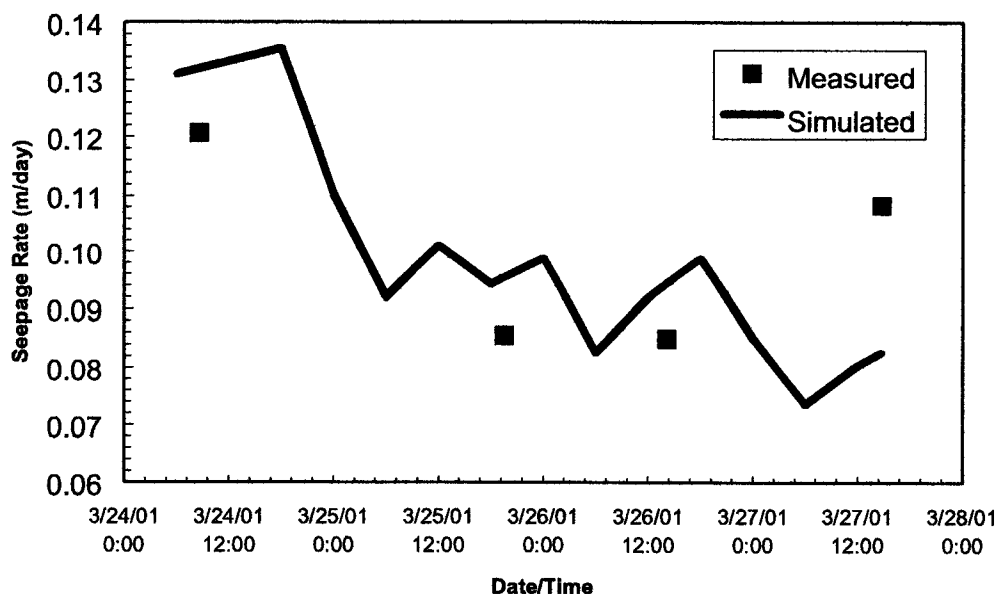
Figure 57. Simulated and measured seepage rate during the ponding experiment.

COMPARISON BETWEEN THE GEOPHYSICAL SURVEY AND THE MODELING AT THE INSTRUMENTED SITES

Saturation potential base on the electrical resistivity survey was one of the main criteria used in site selection with the anticipation of applying the flux rates along the entire canal base on the geophysical survey. Table 3 shows the estimated hydraulic parameters and the saturation potential base on the geophysical survey (Widmer, 2000). It is important to note that the flux defined here is defined as the total fluid flux [L^3/T] transmitted from the canal divided by the cross-sectional area where flux occurs. The cross-sectional area [L^2] is defined as the straight-line distance in which water is in contact with soil times a unit width (because it is a two-dimensional model) parallel to canal flow. Therefore, the fluid flux is in units of L/T.

Table 3.   Hydraulic parameters and flux rates determined by modeling and saturation potential determined by an electrical resistivity survey at monitoring sites along the Truckee Canal.

Site	Flux cm/day	Kx (m/s)	Kz (m/s)	Anisotropy	Saturation Potential
1	20.8	7.3×10^{-6}	2.8×10^{-6}	0.38	Low
2	3.2	1.4×10^{-6}	4.8×10^{-7}	0.36	High
3	16.9	6.9×10^{-6}	1.7×10^{-6}	0.24	Moderate
4	0.6	3.6×10^{-7}	6.7×10^{-8}	0.18	Low
5	47.8	9.8×10^{-6}	3.97×10^{-6}	0.41	High
6	7.7	2.3×10^{-6}	4.9×10^{-7}	0.22	Moderate

From Table 3 it can be seen that at some of the sites there is a good correlation between the saturation potential predicated by the geophysical survey and the flux estimated by the model. However, the geophysical survey predicted that the saturation potential below Site 2 would be high, where the modeling showed that the flux was very low. The soils encountered below Site 2 consisted of fairly moist clays, so although the sediments were

42

saturated, there was very little water movement. Site 1 is in an area that is described as having low saturation potential, where the modeling showed that the seepage rate is relatively high. The resistivity survey shows that at depth at Site 1, there is a relatively high saturation potential even though near-surface conditions have a low saturation potential. Because the two datasets have a discrepancy, additional calibration could be undertaken to resolve the influence of lithology on the geophysical estimates of seepage potential. However, resurveying the canal with a more focused approach towards the canal could provide a more appropriate mapping tool for canal seepage. The geophysical survey was designed to delineate the lithology beneath the canal to a depth of 120 ft or more. It was also to be used in trying to determine depth to groundwater. Consequently, the focus of the survey was not immediately below the canal. To delineate seepage zones, we would simply redesign the survey. This would probably reduce the man-hours spent on a new survey, give much better resolution and reduce the cost for future work.

ESTIMATED FLUX

To estimate total flux from the Truckee Canal in our project area, we applied the modeled flux at each site to a section or an area under the canal. The length for each section includes the space from the midway points between each site. The first and sixth segments include the area from the monitoring site to the midpoint between it and the adjacent site. Canal widths are the average values determined from a minimum of 25 measurements for each section. Table 4 summarizes the values used in the flux determination. These values are presented in English units so that comparisons can be made with other reported values.

Table 4.   Estimated volumetric seepage rates within the study area.

Section	Length (ft)	Length (mi)	Average Channel Width (ft)	Seepage Rate (ft/day)	Volumetric Seepage Rate (ac-ft/yr)
1	3626.5	0.69	61.6	0.68	1272.9
2	6904.0	1.31	68.7	0.11	437.2
3	5827.5	1.10	67.6	0.55	1814.2
4	5230.0	0.99	59.1	0.02	51.8
5	8842.5	1.67	59.4	1.57	6904.0
6	6162.5	1.17	54.8	0.25	707.4
				Total	11,187.

The estimated seepage between Sites 1 and 6 totals 11,187 af/y with an average of 1,614 af/y/mi of canal. This value falls in the middle of the range of values determined by Pohll et al. (2001)

CONCLUSIONS

The model VS2DH was used in conjunction with the parameter optimizer PEST to estimate the hydraulic parameters, hydraulic conductivity and anisotropy, and the flux rates in several locations along the Truckee Canal in the town of Fernley. Measured surface and water temperatures were used as input to VS2DH, while measured subsurface temperatures were used by PEST to refine estimates of the hydraulic conductivity and anisotropy. The estimated seepage rate along the modeled sections of the Truckee canal range from 0.6 to 47.8 cm/day with an average value of 16.2 cm/day (0.02 to 1.57 ft/day and an average of 0.53 ft/day). The total estimated seepage between Sites 1 and 6 is 11,187 af/y, which over the 6.9 miles of canal where the modeling was performed averages 1,614 af/y/mi of canal.

REFERENCES

Carsel, R.F. and R.S. Parrish, 1988. Developing joint probability distributions of soil water retention characteristics. *Water Resources Research*, 24(5):755-769.

Constanz, J., C.L. Thomas and G. Zeueger, 1994. Influence of diurnal variations in stream temperature on streamflow loss and groundwater recharge. *Water Resources Research*, 30(12):3253-3264.

Deutsch, C.V. and A.G. Journel, 1992. GSLIB Geostatistical Software Library and User's Guide, Oxford University Press, New York.

Diersch, H.G., 1998. FEFLOW Reference Manual, WASY Institute for Water Resources Planning and System Research, Ltd., Berlin, Germany.

Healy, R.W. and A.D. Ronan, 1996. Documentation of Computer Program VS2DH for Simulation of Energy Transport in Variably Saturated Porous Media—Modification of the U.S. Geological Survey's Computer Program VS2DT. U.S Geological Survey Water-Resources Investigations Report 96-4230.

Jury, W. A., W.R. Gardner, and W.H. Gardner, 1991. Soil Physics, John Wiley and Sons, New York.

Pohll, G., D. McGraw, J. Ralston, B. Bohm, J. Thomas, A. McKay, M. Widmer, T. Minor, G. Lamorey, O. Dahan, R. Carroll, K. Cupp, E. Jacobson, E. McDonald, E. Stevick and J. Huntington, 2001. Evaluation of Groundwater and Solute Transport in the Fernley – Wadsworth Area. Desert Research Institute Publication No. 41173.

Ronan, A.D., Prudic, D.E., C.E. Thodal and J. Constantz, 1998. Field study and simulation of diurnal temperature effects on infiltration and variably saturated flow beneath an ephemeral stream. *Water Resources Research*, 34(9).

Widmer, M.C., 2000. Unpublished letter to George Ball. Subject Letter Report Geophysical Survey, Truckee Canal.

APPENDIX: TEMPERATURES FROM THERMOCOUPLE ARRAYS AT MONITORING SITES ALONG THE TRUCKEE CANAL